Trends in Analytical Chemistry 195 (2026) 118593

Contents lists available at ScienceDirect

Trends in Analytical Chemistry

journal homepage: www.elsevier.com/locate/trac

Towards clinical application: Emerging strategies for ultrasensitive and selective miRNA detection

Yuhan Wang [a], Zijian Liu [a], Hen-Wei Huang [b], Jung Seung Lee [c], Kexin Liu [a], Mengru Yu [a], Xiaoyue Qi [a,*]

[a] School of Medical Technology, Beijing Institute of Technology, Beijing, 100081, China
[b] School of Electrical & Electronic Engineering, Nanyang Technological University, 639798, Singapore
[c] Department of MetaBioHealth, Sungkyunkwan University, Suwon, 16419, Republic of Korea

A B S T R A C T

MicroRNAs (miRNAs), crucial post-transcriptional regulators, are closely linked to numerous diseases and are emerging as vitally significant biomarkers for ultra-early clinical diagnosis. Driven by advances in precision machining, nanomaterials, and artificial intelligence (AI), miRNA detection is transcending its former limitations to clinical application. This review covers innovative methods developed over the past five years, with a systematic analysis of the enhancement mechanisms, including signal amplification strategies, nanotechnology, clustered regularly interspaced short palindromic repeats and CRISPR-Cas systems, and integrated biosensors. Additionally, integrating advanced technologies such as machine learning, intelligent data processing and algorithms promise to enable more efficient and accurate miRNA detection. The innovative design of these next-generation methodologies effectively surmounts the limitations of conventional assays, achieving remarkable performance benchmarks including ultra-high sensitivity (extending to the attomolar level), exceptional specificity (capable of single-base discrimination), user-friendliness compatible with point-of-care testing (POCT), and even wearability, thereby promoting early diagnosis and personalized medicine.

1. Introduction

MicroRNAs (miRNAs) are a class of non-coding single-stranded small RNAs with a length of approximately 19–23 nucleotides [1]. As of 2024, miRBase has included 1917 precursor miRNAs (pre-miRNAs) and 2654 mature miRNAs [2]. The transcription of miRNAs occurs independently. A single miRNA can regulate up to 100 potential mRNAs targets, and multiple miRNAs can target the same mRNA cooperatively, underscoring their complex regulatory roles in gene expression.

As crucial post-transcriptional regulators, aberrant miRNAs expression correlates with various human diseases, including cardiovascular diseases [3], metabolic disorders [4], neurodegenerative diseases [5], malignant tumors [6], etc. For instance, Zhao et al. [7] demonstrated that miRNA-25802 is significantly upregulated in the plasma of Alzheimer's disease (AD) patients. Notably, in disease progression, the abnormal expression of miRNAs usually precedes changes in related protein markers [8]. Therefore, as early diagnostic biomarkers, miRNAs hold great potential, offering a critical window for early intervention and treatment of diseases.

Traditional miRNA detection techniques include Northern blot, quantitative real-time reverse transcription polymerase chain reaction (qRT-PCR), and microarray technology [9]. Although these methods possess favorable analytical capabilities, their applications are extremely constrained by the inherent limitations and the lack of access to sophisticated instruments outside laboratory settings [10–14]. With the growing demands for higher precision in disease diagnosis and treatment, the current situation significantly hinders the clinical detecting application, and fails to meet the need for rapid and real-time detection to guide clinical decision-making.

Recent advances in miRNA detection have been reported across various technological domains such as plasmon-enchanted biosensors [15], lateral flow assays [16], electrochemical biosensors [17,18], microfluidics [14]. Several reviews have systematically categorized these detection strategies. Gorgani et al. [9] reviewed the application of metal-organic frameworks (MOFs) and their derivatives in miRNA biosensing, covering multiple detection modalities, including fluorescence, electrochemical and luminescence, along with their underlying principles and analytical performance. Jet et al. [19] focused on multiplex miRNA detection technologies, highlighting amplification strategies such as qRT-PCR, rolling circle amplification (RCA), and duplex-specific nuclease signal amplification (DSNSA), as well as platforms enabling simultaneous detection of multiple miRNAs. Their work underlined the capability of these methods to achieve high sensitivity while maintain multiplexing efficiency. However, most published reviews lack fusion

* Corresponding author.
E-mail address: qixiaoyue@bit.edu.cn (X. Qi).

https://doi.org/10.1016/j.trac.2025.118593
Received 22 September 2025; Received in revised form 3 December 2025; Accepted 3 December 2025
Available online 8 December 2025

analysis of multi technologies and a systematic analysis of their core mechanisms, applicable scenarios, and translational potential, as well as a forward-looking discussion of the integration of artificial intelligence (AI) with miRNA detection methods.

After outlining the current challenges in miRNA detection, this review systematically summarizes emerging methodologies with signal enhancement mechanism and offers a comprehensive integration of AI to boost the powerful clinical application. By analyzing their performances, advantages, and limitations, we discuss how these innovations overcome the drawbacks of conventional approaches to achieve more efficient, sensitive, and accessible detection. Subsequently, this review analyzes the mechanisms of high sensitivity and specific selectivity and then presents a forward-looking perspective on the integration of AI in miRNA detection.

2. Challenges in miRNAs detection

miRNAs are short-sequence molecules [1] with extremely low abundance in biological samples. This inherent characteristic leads to challenges in detection, including low sensitivity, poor specificity, lengthy procedures, and complex sample processing.

(i) Hysteresis detection. Traditional miRNA detection methods include Northern blot, qRT-PCR, and microarrays. Workflows are generally labor-intensive and time-consuming, involving extraction, purification, reverse transcription, amplification, and signal detection with increased cost and miRNA loss risk or degradation, .e.g. several hours for qRT-PCR results coming out, hindering point-of-care testing (POCT) efficiency [14].

(ii) Low sensitivity. miRNAs in biofluids like urine, saliva, and serum exist at very low concentrations—often the fM levels [20]. qRT-PCR offers good specificity for known miRNAs, yet its amplification efficiency for low-abundance targets is suboptimal, resulting in inconsistent sensitivity and quantification inaccuracies.

(iii) Insufficient throughput. Diseases may be closely related with multiple miRNAs [21] as they influence diverse physiological and pathological processes through intricate regulatory pathways, including biological development, organ formation, hematopoiesis, viral defense, and lipid metabolism. However, traditional detection methods mostly target single miRNA, making it difficult to achieve high-throughput and multiplex detection.

3. Novel strategies for highly sensitive miRNAs detection

3.1. Nucleic acid-based signal amplification strategies

3.1.1. Rolling circle amplification (RCA)

RCA is known for its simple, efficient, and robust isothermal nucleic acid amplification technology. A typical RCA system requires four

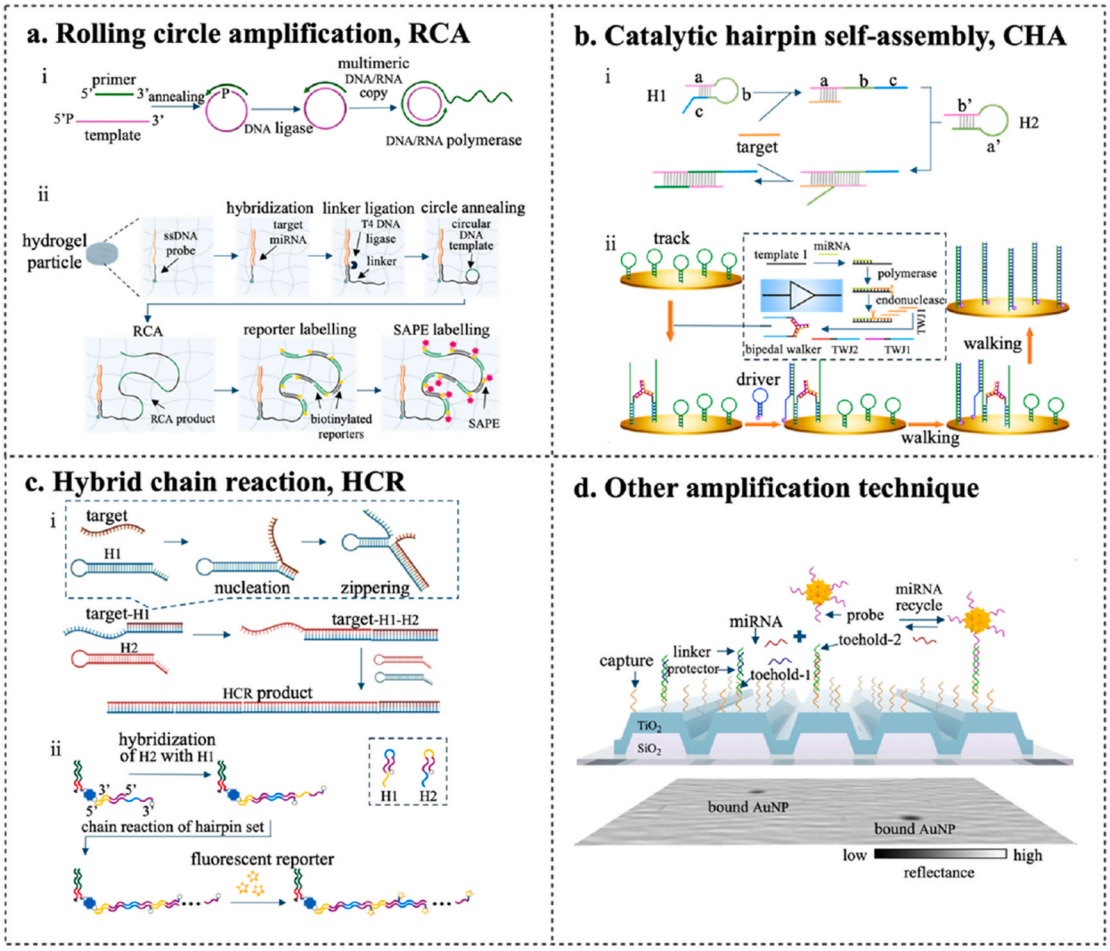

Fig. 1. Nucleic acid-based signal amplification strategies. a) Rolling circle amplification: i) The basic reaction process of RCA. Copyright 2021, Elsevier [22]; ii) miRNA capture and detection in encoded hydrogel microparticles. Copyright 2022, Wiley-VCH GmbH [24]. b) Catalytic hairpin self-assembly: i) The basic reaction process of CHA. Copyright 2023, Elsevier [29]; ii) Bipedal DNA walking based electrochemical detection of miRNA. Copyright 2021, American Chemical Society [32]. c) Hybrid chain reaction: i) The basic reaction process of HCR. Copyright 2025, Wiley-VCH GmbH [33]; ii) Hydrogel-based HCR amplification. Copyright 2021, Elsevier [35]. d) Other amplification technique: based on TRAP and photon resonator absorption microscopy. Copyright 2023, Wiley-VCH GmbH [38].

essential components: (1) a circular DNA template, (2) a short DNA primer or RNA promoter, (3) deoxynucleotide triphosphates (dNTPs) or nucleotide triphosphates (NTPs), and (4) DNA/RNA polymerase (Fig. 1a (i)) [22]. Specifically, DNA/RNA polymerases with strand displacement activity are used to extend primers. They base on template sequences to generate long single-stranded DNA or RNA nanowires containing hundreds of tandem repeats. The length of RCA products can be controlled by adjusting the dNTPs/NTPs concentration, the DNA/RNA polymerase concentration or the reaction time [23].

Al Sulaiman et al. [24] realized quantitative and multiplex detection of extracellular vesicle-derived microRNAs (EV-miRNAs) by performing RCA within encoded hydrogel particles. This method integrates one-pot extracellular vesicle lysis and miRNA capture steps, achieving a limit of detection (LOD) as low as 0.046 fM (Fig. 1a (ii)). The innovative combination of encoded hydrogel particles and RCA technology effectively solves the problem of cumbersome steps and high error susceptibility in EV-miRNA detection. However, the complicated preparation process of hydrogel particles may restrict the large-scale clinical application. Moreover, RCA technology can be used for simultaneous miRNAs and message RNAs (mRNAs) detection at single-cell level in plant tissues [25]. This method has undergone quantitative and numerical testing in transgenic rice with different gene expression levels, expected to serve as a sensitive and versatile technique for investigating miRNA-regulated plant tissue.

The RCA technique shows a good detection effect, and integrating RCA with other technologies can further improve sensitivity and selectivity. It can even achieve multi-target detection. In 2022, Zhang's group innovatively integrated primer generation-mediated rolling loop amplification (PG-RCA) with primer exchange reaction (PER) [26], and combined exponential rolling loop amplification (EXP-RCA) [27] with linear rolling loop amplification (LRCA), respectively. The LOD of these strategies can reach aM level and distinguish non-target miRNAs with single base mutation. In addition, focusing on the detection of multiple miRNAs, the same group [28] fabricated a multicolor fluorescent aptamer sensor based on rolling circle transcription amplification (RCTA) and fluorescent light-up aptamers (FLAPs), which can simultaneously detect multiple miRNAs in breast cancer tissues. The LOD of three related miRNAs reached aM level, and it shows no response to irrelevant miRNAs. All strategies address the limitation of requiring expensive labeling and auxiliary primers, offering advantages such as high amplification efficiency. It requires no complex modification or separation steps, permitting direct, ultra-highly sensitive, and specific miRNA detection.

RCA has showed unique advantages in miRNAs detection, but it requires the participation of enzymes. This phenomenon leads to a longer enzymatic reaction time in the cycle, which greatly affects the POCT. Therefore, to overcome the time limit and meet the real-time detection, enzyme-free amplification technology can be used as one of the breakthrough points.

3.1.2. Catalytic hairpin self-assembly (CHA)

CHA shows great potential in improving sensitivity due to its advantages of high efficiency, non-enzyme, isothermal amplification, flexible deign and low cost (Fig. 1b (i)) [29]. A typical CHA involves an initiator (C1) and two DNA hairpins (H1, H2) that remain stable without C1. Upon C1 addition, H1 is unfolded as the complementary region of C1 hybridizes with the exposed toehold H1, forming an intermediate product of H1–C1 complex. Subsequently, the exposed part of H1 reacts with H2 again, and H2 is unfolded accordingly to form an H1/C1/H2 complex. Finally, the newly released H2 initiates branch migration, leading to C1 release and stable H1–H2 double-stranded DNA (dsDNA) formation. The released C1 can trigger next cycle of CHA, further amplifying the signal [30].

Yang et al. [31] developed a signal amplifier-assisted DNA "AND" logic gate combined with the CHA strategy for simultaneously detecting three acute myocardial infarction (AMI)-related miRNAs (miRNA-133a, miRNA-499, miRNA-21). When all three miRNAs present, they bind to their corresponding duplexes respectively, releasing single-stranded DNA (ssDNA) (T1, T2 and T3), which hybridize with S1, S2 and S3, leading to the release of S4. The released S4 then initiates CHA reaction causing 6-carboxyfluorescein (FAM) and black hole quencher 1 (BHQ1) to separate and fluorescence to be enhanced. This method can effectively distinguish non-target miRNAs with a low LOD at the pM level and a wide detection range spanning from 0.05 to 20 nM.

Building upon traditional CHA principle, Miao et al. [32] constructed a DNA logic system based on cascaded strand replacement with a bipedal DNA walker further lowering the LOD to aM level since this bipedal walker contains a three-way junction structure, which can catalyze the simultaneous opening of two hairpins on adjacent track sequences (Fig. 1b (ii)). Building on this foundation, a full series of Boolean logic gates are designed, including: (i) Single-input gates: the YES gate (for single miRNA detection) and the NOT gate (with inverted input-output relationship); (ii) Dual-input gates: the AND, OR, NAND, NOR, XOR, and XNOR gates (using miRNA-21 and miRNA-20a as inputs); (iii) Three-input gates: the AND/OR gates (using miRNA-21, miRNA-20a, and miRNA-106a as inputs). Currently, this technology has only been preliminarily tested in cells and human tissue samples. In practical clinical applications, the impact of the biological samples complexity on experimental results needs to be considered.

3.1.3. Hybrid chain reaction (HCR)

HCR is an enzyme-free amplification strategy that uses a set of DNA hairpins under isothermal conditions. HCR amplification is based on conventional DNA hybridization, requiring at least two partially complementary DNA hairpins that should coexist in a metastable state [33]. When the initiator hybridizes with target, its 5′ and 3′ ends become available and hybridize with H1. In this process, H1 is still a single-stranded part complementary to H2. So H2 is unfolded and binds to H1, leading to continuous polymerization of H1 and H2, which triggers signal amplification (Fig. 1c (i)). Morihiro et al. [34] constructed a nucleic to small molecule converter combining CHA and HCR. In this system, fluorophores and dye molecules are released in response to miRNA-21 through HCR, providing fluorescent and colorimetric readouts. Meanwhile, CHA can kill cells selectively with abundant miRNA-21 and release the anticancer drug SN-38. This method innovatively integrated HCR and CHA to achieve dual effects of detection and therapy. It is the first example of selective activation of small molecule prodrugs triggered by oncogenic miRNA in living human cells. Moreover, researchers [35] also designed a hydrogel-based HCR for detecting urinary exosomal miRNAs in human clinical samples (Fig. 1c (ii)). Leveraging the three-dimensional structure of hydrogel and signal amplification capability of HCR, this approach has successfully detected a small amount (~amol) of exosomal miRNAs from 600 μL urine. This approach can be used as a novel diagnostic platform for non-invasive liquid biopsy before cumbersome tissue biopsies for various diseases, including prostate cancer screening, complementing prostate-specific antigen (PSA) testing. It was the first report at that time to analyze exosomal miRNAs in less than 1 mL of urine without target amplification.

3.1.4. Other amplification techniques

Beyond the signal amplification methods, researchers have also actively explored new breakthroughs and employed alternative approaches to amplify signals. Most amplification technologies require the involvement of enzymes. To improve detection efficiency, Wang et al. [36] constructed a dual-cycle system (cyclic strand displacement amplification and cyclic exonuclease cleavage), which finally induced cyclic exponential amplification. This process leads to the release of many 2-aminopurine (2-AP) molecules, thereby generating a fluorescent signal (without a fluorescent quencher). This method exhibits an eight-fold dynamic range and ultra-high sensitivity, with a LOD of 0.16 aM. In terms of selectivity, it can distinguish single-base mismatches in

miRNA-486-5p and this method enables accurate quantification of miR-486-5p across different stages of lung cancer cells. In contrast to the reported methods for miRNA assay, this method achieves exponential signal amplification through a rapid, one-step, isothermal, and label-free process. More importantly, the proposed method can be applied to accurately quantify miRNA-486-5p in lung cancer cells at various stages, and even distinguish the expressions of circulating miR-486-5p in healthy persons from those in non-small-cell lung carcinoma patients, holding great promise in biomedical research and clinical diagnosis. Furthermore, enzyme-free amplification approaches can further simplify detection procedures and enhance detection stability. The Janus hydrogel fuel stimulant-powered (FSP) amplification technology, relying on fuel-assisted DNA cascade reactions without temperature control and nucleic acid amplification enzymes, can be used for simultaneous miRNA-125b and miRNA-21 detection [37]. This method was the first reported application of Janus hydrogel-based FSP amplification technology for detecting gastric cancer related miRNAs. Moreover, Wang et al. [38] reported a digital detection method for exosomal miRNAs based on target recycling amplification process (TRAP) and photon resonator absorption microscopy (Fig. 1d). It enables multiplex detection with 20 min, and the LOD for miRNA-275 and miRNA-21 are 0.24 aM and 0.356 aM, respectively. Compared with traditional qRT-PCR, TRAP exists similar accuracy, but it improves LOD by 31-fold and 61-fold, respectively, providing a simpler method for early cancer detection. Duplex-specific nuclease (DSN) can specifically recognize and cleave the DNA strand in DNA-RNA heteroduplexes, while having no significant cleavage effect on ssDNA, single-stranded RNA (ssRNA), or dsDNA. Taking advantage of this feature, Lei et al. [39] developed dual-surface-protein-guided orthogonal recognition of tumor-derived exosomes and in situ probing of miRNA (SORTER) profiles for rapid and specific detection of tumor-derived exosomal miRNAs. DSN-mediated signal amplification is one of the core technologies. When the recognition sequence on gold nanoflares (AuNFs) binds to the target miRNA in exosomes to form a DNA-RNA heteroduplex, DSN specifically cleaves the DNA sequence in this heteroduplex, releasing the fluorophore to generate a fluorescent signal. At the same time, the released RNA sequence can bind to the recognition sequences on other AuNFs again, initiating the target recycling and signal amplification process. This method offers excellent analytical performance for liquid biopsy applications, consuming only 0.2 μL plasma sample and completing the entire analysis in less than 2 h. Notably, it achieves 100 % sensitivity, specificity, and accuracy in differentiating prostate cancer and benign prostatic hyperplasia.

Due to the short nucleotide sequences, low abundance in biological samples and susceptibility to interference from background substances, miRNAs pose challenges to traditional detection methods. Single amplification techniques, including RCA, CHA, HCR, etc., provide effective solutions for miRNAs detection. Nevertheless, these technologies still have limitations. For instance, RCA relies on enzymatic reaction, which is not only time-consuming but also the enzyme activity is easily affected by pH and temperature in systems. These characteristics result in poor experimental repeatability. Although CHA and HCR are enzyme-free, they require highly precise hairpin design and are susceptible to stability, which may lead to false triggering and false positive results. In addition, some technologies, such as hydrogel-based detection methods, involve complex material preparation processes, making it difficult to achieve rapid mass production. In the future, efforts can be made to develop more efficient amplification technologies, by integrating microfluidics, nanomaterials, and others to achieve POCT for miRNAs.

3.2. Nanomaterials-facilitated signal enhancement

Nanomaterials, which exhibit unique optical, electrical, and physicochemical properties, significantly enhance sensitivity and selectivity in bioanalysis, supporting improved disease diagnosis and biomolecular research.

3.2.1. Fluorescence detection mechanism

Nucleic acid templated-silver nanoclusters (NA/AgNCs) are silver nanoclusters (AgNCs) stabilized by nucleic acids as ligands, constituting a class of fluorescent carriers exhibiting photophysical and photochemical properties [40]. Among them, DNA-encapsulated silver nanoclusters (DNA/AgNCs) demonstrate large Stokes shifts, tunable emission colors, brightness and photostability, thus being widely used in finding extensive application in biomolecular detection. Yadavalli et al. [41] developed a novel Tail-Hoogsteen triple-layered DNA/AgNCs system for miRNA detection (Fig. 2a (i)). Upon binding target miRNAs, the system switches from low to red fluorescence, enabling “on” mode detection suitable for real-time monitoring, requiring no costly labels or enzymes.

Furthermore, combining dual nanomaterials can further improve detection sensitivity and specificity. A dual-nanoparticle system composed of polystyrene and SiO_2 (labeled by Cy5 and Cy3, respectively) enables single-base-specific detection of miRNA-122 [42], achieving a LOD over 2000-fold lower than previous methods. When Cy5/Cy3 is detected at the same time, the presence of target miRNA-122 in the sample can be confirmed, which can significantly improve the accuracy of the detection. However, these methods mainly focus on single marker detection, resulting in low detection throughput.

As a new type of fluorescent material, quantum dots (QDs) have obvious advantages such as strong intensity, high stability, strong antibleaching ability, broad excitation spectrum, narrow emission spectrum, and tunable emission wavelength [43,44]. The quantum dot-molecular beacon functionalized MoS_2 (QD-MB@MoS_2) fluorescent probe was first reported in 2022 [45] for simultaneous detection of myeloma-associated miRNA-155 and miRNA-150 (Fig. 2a (ii)). The LOD for two miRNAs in human serum were as low as 7.19 fM and 5.84 fM, respectively. However, it relies on DSN recognize and cleave DNA, rendering it susceptible to the factors such as temperature and pH. Based on this, a QD-based nano-sensor was demonstrated by Ma et al. [46], enabling simple and sensitive detection of miRNA at the fM concentration range without requiring any enzymes. To further improve detection efficiency, Xiong et al. [47] used photonic crystal (PC) surfaces, achieving nearly 3000-fold signal enhancement through multiple mechanisms: surface enhanced excitation, highly directional emission extraction, improved quantum efficiency, and blinking suppression. This platform demonstrated an LOD of 10 aM for miRNA-375, with a good linear dose-response relationship from 10 aM to 1 nM. Only using low-cost optical equipment, this method provides digital resolution of single molecules for highly specific, wide dynamic range, rapid, and clinically relevant atomic miRNAs detection. However, the fluorescent label itself is susceptible to environmental interference and spectral overlap. In the future, it is necessary to further optimize.

Furthermore, researchers have also devoted nanoparticle-based integrated diagnosis and treatment platform [48], which realizes miRNAs guided cancer cell imaging and therapy. In the future, this concept can be extended to image and photodynamic therapy of any other diseased cells with overexpressed miRNAs by modifying other recognition sequences (like biomarker specific aptamers) into hairpin structural domains.

3.2.2. SERS detection mechanism

Compared to fluorescence methods, surface-enhanced Raman spectroscopy (SERS) has the advantages of ultrahigh sensitivity, narrow peak width, low background signal, and inherent chemical fingerprint information [49].

Raman spectroscopy is well-suited for multiplex miRNA detection, with SERS offering strong signal amplification by leveraging the plasmonic properties of metal nanostructures. The SERS effect combines electromagnetic and chemical enhancements: under light excitation, surface plasmon resonance amplifies the local electromagnetic field,

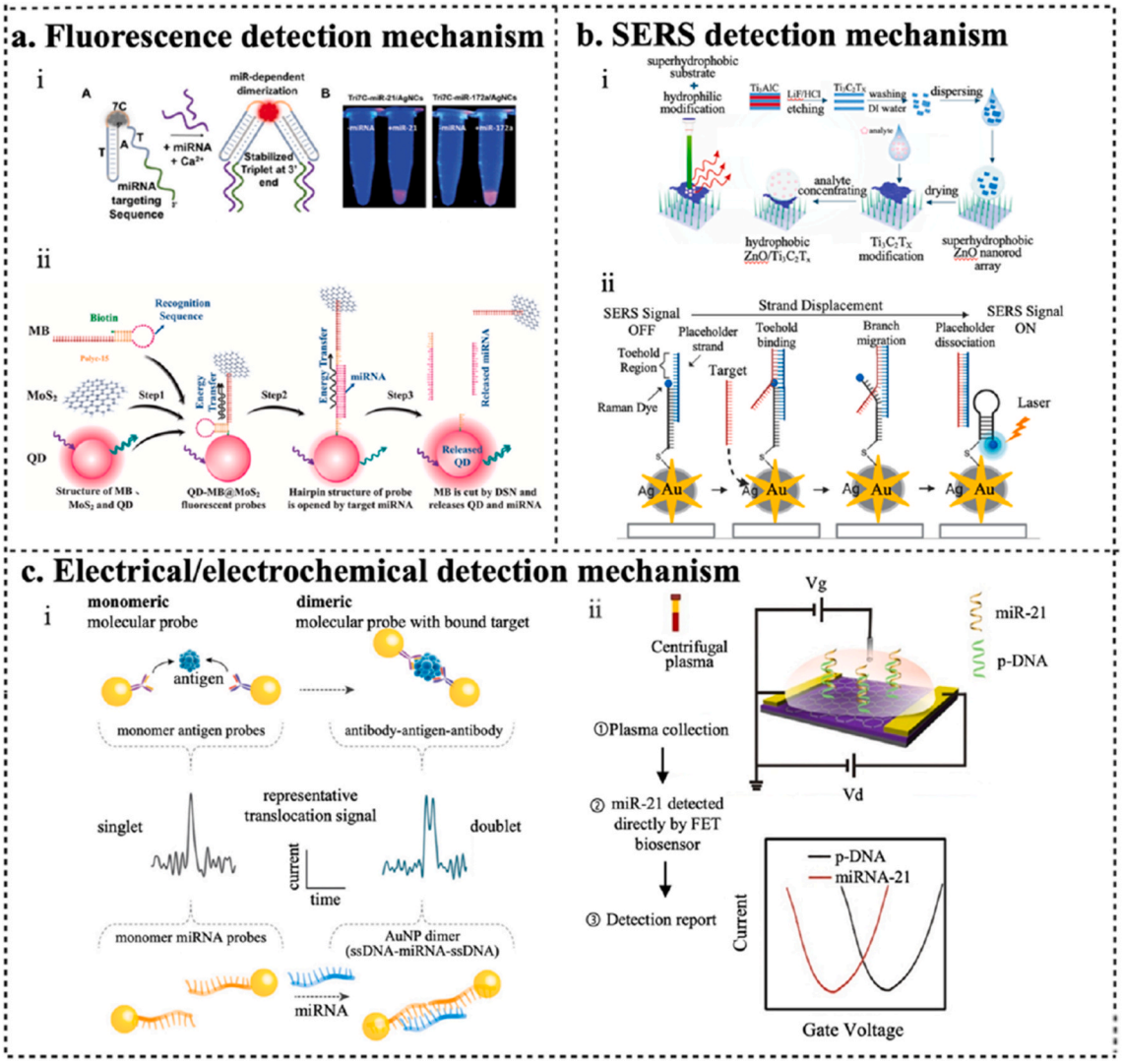

Fig. 2. Nanomaterials-facilitated signal enhancement technologies. a) Fluorescence detection mechanism nanoparticle: i) The increased fluorescence intensity of Hoogsteen triplex DNA/AgNCs sensors due to the binding of miRNA. Copyright 2023, Wiley-VCH GmbH [41]; ii) Dual miRNA detection by QD-MB@MoS_2 fluorescent probes. Copyright 2022, KeAi Communications [45]. b) SERS detection mechanism: i) miRNA detection based on ZnO/$Ti_3C_2T_x$ substrate and SERS. Copyright 2022, American Chemical Society [48]; ii) Illustration of miRNA detection based on the iMS probe assay and SERS mechanism. Copyright 2023, Elsevier [52]. c) Electrical/electrochemical detection mechanism: i) miRNA detection by monomeric and dimeric NPs. Copyright 2021, Wiley-VCH GmbH [57]; ii) Schematic of the FET combined with RGO of miRNA detection for breast cancer patients. Copyright 2022, ACS Publications [58].

boosting the Raman signals of nearby molecules [50]. Integrating various nanoparticles further enhances SERS detection performance. Wu et al. [51] innovatively deposited hydrophilic $Ti_3C_2T_x$ films onto superhydrophobic ZnO nanorod arrays to obtain a SERS substrate with higher affinity (Fig. 2b (i)). But this method may encounter differential absorption of nucleotide bases (such as U and A) on substrate, leading to variations in Raman signal intensities. This affects the accuracy, stability, and quantitative precision of biomolecular measurements. To simultaneously leverage the advantages of SERS and metal nanomaterials, a SERS platform based on bimetallic nano-stars for miRNAs detection has been developed [52]. By optimizing integration of inverse Molecular Sentinel (iMS) gene probes on this platform, it achieves ultrasensitive detection of two miRNAs, enabling effective discrimination between samples from healthy individuals and cancer patients (Fig. 2b (ii)). SERS-based optical detection is excellent in terms of multiplexing capabilities and the specificity of miRNA analysis, but this method relies on complex light sources or signal amplification substrates.

3.2.3. *Electrical/electrochemical detection mechanism*

Electrical and electrochemical detection methods are known to be simpler and to require mostly inexpensive simple electronics. Compared with most optical detection technologies, electrochemical methods are insensitive to stray light and applicable to turbid samples [53]. Due to their high sensitivity, low LOD, cost-effectiveness and capability for large-scale production, electrical and electrochemical detection methods have garnered significant interest [54,55]. In recent years, several studies have focused on utilizing electrical or electrochemical methods combined with nanomaterials for miRNAs detection.

Gold nanoparticles (AuNPs) can be used for miRNAs detection due to their excellent electrical conductivity, outstanding electron transfer capability, good biocompatibility, and high stability (Fig. 2c (i)) [56]. Ren et al. [57] achieved protein (procalcitonin, a biomarker of sepsis) and miRNA (miRNA-141-3p, a potential indicator of prostate cancer) detection at the single-molecule level by distinguishing the differences between single peaks (monomers) and double peaks (dimers) in ionic current signals via nanopores. This strategy can efficiently distinguish miRNA-141 and miRNA-200a, which differ by only two nucleotides.

However, the LOD of miRNA has reached at the pM level and still needs further optimization. Moreover, owing to its two-dimensional structure of carbon atoms joined by covalent σ-bonds, graphene oxide (GO) exhibits exceptional mechanical strength, a large specific surface area, outstanding electrical properties, and high charge carrier mobility. The field effect transistors modified with reduced graphene oxide (RGO-FET) has become a powerful platform for miRNA detection, due to its advantages of ultrasmall size with high sensitivity, high selectivity, fast analysis, and label-free characteristics (Fig. 2c (ii)) [58]. This method can achieve a LOD of 1 fM for miRNA-21 and can distinguish between perfectly matched, single-base mismatched and perfectly mismatched sequences. The above detection methods can achieve target miRNA detection without requiring extraction, amplification, and labeling during the process.

In addition to traditional nanomaterials, the integration of advanced functional materials such as carbon nanofibers (CNFs) has emerged as a promising choice for the development of electrochemical biosensing, owing to their exceptional electrical, mechanical, and chemical properties. Sharama et al. [59,60] reported a sensing platform based on electrochemistry, which integrated carbon nanofibers to detect miRNA-21 (LOD: 9.42 aM). Notably, researchers investigated the charge transfer mechanism of this method through COMSOL Multiphysics and found that the enhanced sensitivity is mainly attributed to the improved electrical conductivity, surface area, and surface chemical properties induced by functionalized CNFs.

Nanomaterials have been widely applied in miRNA detection, with some achieving integrated diagnosis and therapy. Future directions include optimizing synthesis and modification for greater stability and performance (e.g., reducing QD fluorescence intermittency, improving superhydrophobic substrates), developing multiplexed miRNA detection methods, and integrating nanomaterials with technologies such as AI and microfluidics to enable miniaturized, intelligent, and automated detection with improved accuracy and convenience.

3.3. CRISPR-cas system

The CRISPR-Cas system is an adaptive immune mechanism present in prokaryotes. Due to its programmable ability to accurately cleave specific nucleic acids [61], it is widely applied in genome editing, gene expression regulation, biosensors, and other fields [62]. Following CRISPR-associated protein 9 (Cas9), CRISPR-associated protein 12a (Cas12a) and CRISPR-associated protein 13a (Cas13a) have expanded the scope of CRISPR technology. Cas12a and Cas13a possess the ability to bind single-stranded guide CRISPR RNA (crRNA) [63]. They can cleave dsDNA and double-stranded RNA (dsRNA), respectively (called *cis*-cleavage). And they are also possible to indiscriminately digest nearby non-target ssDNA and ssRNA (called *trans*-scission), enabling targeted editing of DNA and RNA.

3.3.1. CRISPR-Cas with reverse transcription

Over the past decade, CRISPR-Cas-based miRNA detection has advanced significantly; however, due to miRNAs' short length and absence of native protospacer adjacent motif (PAM) sequences [64], reverse transcription into DNA is typically required for detection.

Jia et al. [65] constructed a programmable miRNAs detection platform by integrating CRISPR-Cas12a with HCR circuit (Fig. 3a (i)). A hairpin probe H1 containing a specific loop region recognizes miRNAs, triggering HCR to generate dsDNA containing PAM sequences. Then it activates *trans*-cleavage activity of Cas12a. Cellular experiments showed that this method achieved a LOD of 1 fM for miRNA-21, with a linear range covering 10 orders of magnitude amazingly. Moreover, by adjusting the variable region of H1, this method can achieve detection of

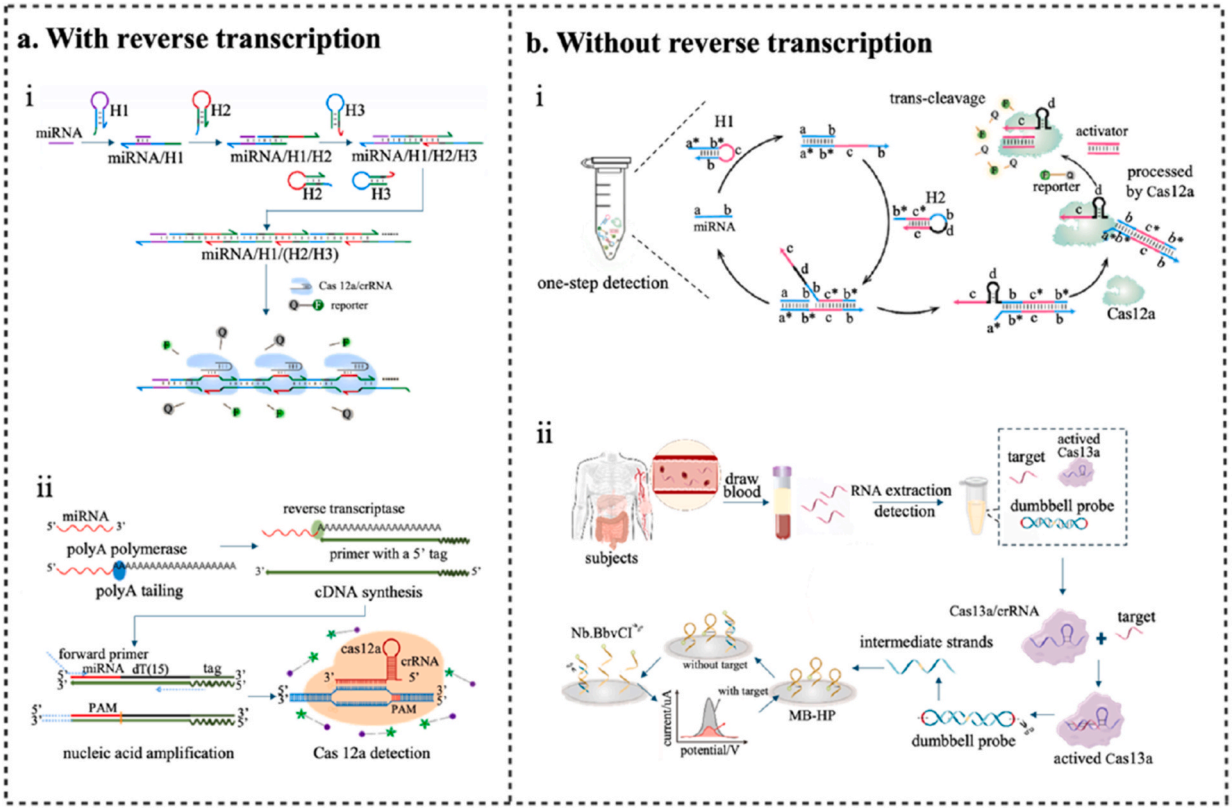

Fig. 3. CRISPR-Cas system strategies. a) With reverse transcription: i) Schematic illustration of the CRISPR-HCR for miRNA detection. Copyright 2022, Elsevier [65]; ii) Workflow of polyA-CRISPR/Cas12a miRNA detection. Copyright 2022, Elsevier [64]. b) Without reverse transcription: i) One-step miRNA detection with Cas12a. Copyright 2022, Elsevier [66]; ii) Schematic illustration of the DP-bridged Cas13a electrochemical biosensor for the detection of miRNA and diagnosis. Copyright 2025, Elsevier [69].

different miRNAs. Notably, this platform amplifies miRNA-specific signals rather than miRNA themselves, avoiding cross-contamination from pre-amplification. However, this system still faces PAM restrictions in application and its single-base specificity detection still needs to be improved. To address this limitation, researchers [64] proposed a polyA-CRISPR/Cas12a miRNAs detection (PCDetection) strategy, which successfully overcomes PAM restriction of Cas12a through polyA tail extension and recombinase polymerase amplification (Fig. 3a (ii)). This method enables specific identification of nucleic acid sequences with single base mismatches. Compared with traditional methods, through a unified polyA tail strategy, PCDetection significantly expanded the application range of CRISPR-Cas system by increasing proportion of detectable miRNAs from 24 % to 100 %. Nevertheless, this method still faces the fundamental challenge of requiring miRNAs reverse transcription to DNAs.

3.3.2. CRISPR-Cas without reverse transcription

Although CRISPR-Cas systems enhance miRNA detection sensitivity and specificity, the need for reverse transcription complicates the clinical translation. Developing CRISPR-Cas systems that directly detect miRNAs is therefore crucial. To address this problem, Chen et al. [66] developed a one-step detection platform combining RNA-based CHA circuits with CRISPR-Cas12a (Fig. 3b (i)). After binding to target miRNAs, this platform can specifically trigger RNA-based CHA circuits, inducing a conformational change in blocked crRNAs to form pre-ribosomal RNAs (pre-rRNAs). These pre-rRNAs can be processed into mature crRNAs, which function by using inherent ribonuclease activity of Cas12a. The LOD for let-7a reaches 81.96 fM. By adjusting the loop region sequence of hairpin H1, it enables adapt to different miRNAs, improving detection flexibility. Compared with conventional CRISPR detection methods, this platform is a single, one-step reaction system only involving one Cas12a protein without reverse transcription, however, there is still room for optimization in terms of sensitivity and selectivity. Jiang et al. [67] developed a dual-functional dumbbell probe-based fluorescent biosensor by integrating PER with the CRISPR-Cas12a system. Notably, this method can achieve a LOD at 0.45 fM and distinguish single-base mismatches as well. Subsequent strategies combining Cas12a/Cas13a with dumbbell [68,69], padlock [70], and *o*-nitrobenzyl phosphate-caged RNA hairpin probes [71] further improved efficiency and flexibility (Fig. 3b (ii)).

Furthermore, these new detection methods can not only detect nucleic acid substances, but also can achieve dual detection of nucleic acid substances and non-nucleic acid substances. Wang et al. [72] designed a programmable DNA nano-switch to regulate plasmonic CRISPR/Cas12a-Gold nanoparticle platform. This platform achieves detection of nucleic acid (miRNA-375) and non-nucleic acid (PSA) markers related to prostate cancer. However, this system can only measure the two targets separately by replacing corresponding nano-switch during detection. It cannot detect two targets at the same time.

In summary, the CRISPR-Cas system shows great promise for miRNA detection due to its precise nucleic acid cleavage and versatile detection strategies. However, challenges remain, including improving single-base specificity, enabling multiplex detection, and addressing clinical barriers such as standardization, cost, and procedural simplicity. Future progress will rely on integrating CRISPR-Cas with other technologies to develop efficient, user-friendly, and broadly applicable platforms, ultimately advancing accurate and automated miRNA diagnostics. To better achieve miniaturization and POCT, integrated biosensors offer the possibility.

3.4. Multitechnology synergy in integrated biosensors

Biosensors have advanced through multidisciplinary integration, achieving high sensitivity and specificity in miRNA detection by combining various technologies. Among them, optical and electrochemical biosensors are the most studied. Optical biosensors include fluorescence, absorption spectroscopy, surface plasmon resonance (SPR), and optical fiber sensors. Electrochemical biosensors detect miRNA through specific interactions on electrode surfaces, producing measurable electrical signals offering stable performance, low cost, ease of use, and miniaturization with great potential in wearables.

3.4.1. Microfluidics

Microfluidics enables integrated, miniaturized biomarker detection for POCT by processing and analyzing samples on micro-structured chips [73]. To enhance miRNA detection, researchers combine microfluidics with signal amplification [74], nanomaterials [75], CRISPR-Cas systems [76], and electrochemical methods [77].

Incorporating signal amplification technologies into microfluidic chips significantly enhances detection sensitivity and efficiency, enabling accurate identification of low-abundance biomarkers. Recent research has further integrated strategies such as HCR, cascade signal amplification, and RCA into microfluidic platforms for highly sensitive, rapid miRNA detection. Zhao et al. [74] developed a shape-encoded hydrogel microparticle system for multiplex miRNA detection, combining probe-loaded particles with HCR signal amplification. Photo-polymerized hydrogel microparticles incorporated acrylate-modified probes into their three-dimension (3D) networks, with each shape corresponding to a specific miRNA target. The target binding initiated HCR using FAM-labeled hairpin probes, depositing fluorescence within the particles. These particles were injected into a custom polydimethylsiloxane (PDMS) microfluidic chip with a microfilter chamber, where accumulated particles acted as parallel microreactors under continuous flow, enabling multiplexed detection in a single channel. Testing in fetal bovine serum achieved LODs of 27.8 pM (miRNA-21) and 24.7 pM (miRNA let-7a). This method is highly specific and can identify single base mismatches. The microfluidic approach significantly increased throughput, reduced detection time, and streamlined operations. While effective, the LOD remains relatively high; sensitivity could be improved by cascading additional amplification strategies.

Fluorescent DNA hairpin probes were designed combined nucleic acid amplification with microchip electrophoresis (MCE) for cascade signal enhancement [78]. A microfluidic chip was employed to achieve single-cell analysis and applied laser-induced fluorescence to quantify miRNA-21 and miRNA-141 level, revealing distinct miRNA expression profiles at the single-cell level. By changing the base sequence of hairpin probes, it can also be applied in simultaneous quantification of other miRNAs in different kinds of single cells which offeres insights into cell proliferation, division, and apoptosis.

The detection of exosome miRNAs can also be achieved on the microfluidic platform, which consists of two separate chips for enrichment and detection, respectively (Fig. 4a (i)) [79]. The miRNAs detection chip can detect up to 8 different miRNAs via on-chip multiplex EXPAR and a low-cost Internet of Things (IoT) reader. Microfluidics with higher precision and better fluid flow control can automate exosome miRNAs detection in the future. Moreover, multiple amplification can be incorporated in a microfluidic sensor, e.g. RCA combine tyramine signal amplification (TSA), to increase the accuracy [80].

In addition to the integration with amplification technology, the combination of microfluidic and nanomaterials has demonstrated significant advantages and greatly improved detection performance, including laser-induced graphene (LIG) [81] (Fig. 4a (ii)) and graphene oxide (GO) [75]. The functionalized microfluidics enabled simultaneously detection of multiple miRNAs (up to 20) within in 35 min, requiring only 2 μL sample, with a LOD as low as 0.146 aM, and it can successfully distinguish non-target miRNAs with double base mismatch and single base mismatch.

A single-mode detection struggles to balance efficiency and accuracy. Therefore, researchers developed a dual-signal microfluidic paper-based device (μPAD) using Bi_2S_3@MoS_2 nanoflowers and octahedral

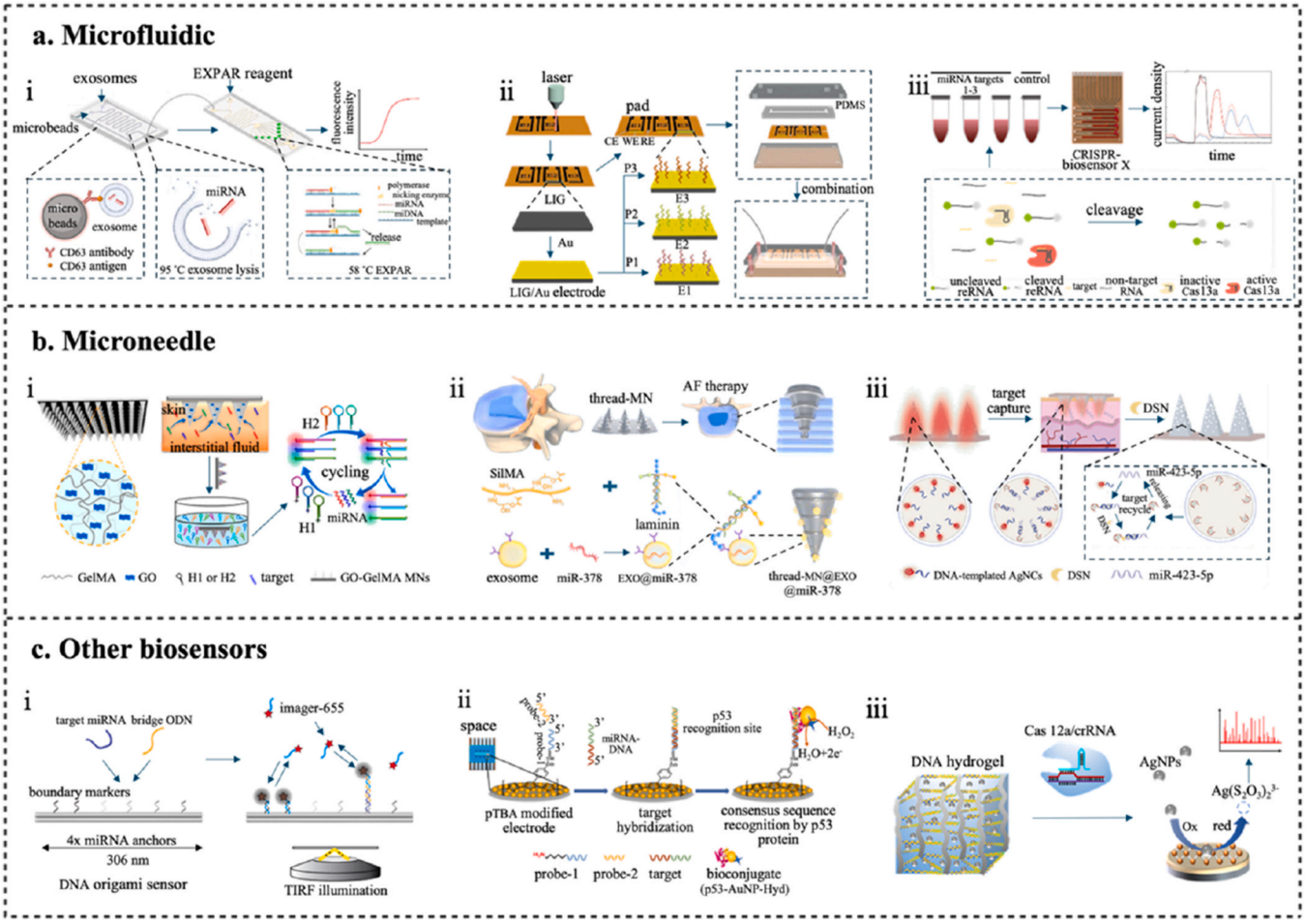

Fig. 4. Multiple biosensors. a) Microfluidic: i) Schematic diagram of the on-chip exosomal miRNA analysis assay. Copyright 2021, Elsevier [79]; ii) miRNA detection with LIG/Au sensing electrodes. Copyright 2024, Elsevier [81]; iii) The amplification-free and simultaneous quantification of up to eight miRNAs on the CRISPR-Biosensor. Copyright 2019, Wiley-VCH Verlag GmbH [84]. b) Microneedle: i) Schematic illustration of GO-GelMA MNs used for ISF extraction and miRNA detection. Copyright 2022 American Chemical Society [89]; ii) Schematic illustration of AgNCs-decorated porous microneedles coupling DSN-assisted signal amplification for ISF miRNA detection. Copyright 2024, KeAi Communications [100]; iii) miRNA detection with a thread-structural microneedle. Copyright 2024, American Chemical Society [91]. c) Other biosensors: i) Electrochemical detection of target miRNAs on the sensing probe modified on the SPACE with p53-AuNP-Hyd bioconjugate. Copyright 2022, Elsevier [104]; ii) miRNA detection with a DNA origami nanoarray system. Copyright 2022, Elsevier [109]; iii) A novel Nano-impact electrochemistry sensing strategy amplified by the CRISPR-responsive DNA hydrogel and cascade DNA assembly. Copyright 2023, American Chemical Society [110].

CeO_2 [82]. The electrochemical mode employed in-situ hydrothermally assembled Bi_2S_3@MoS_2 on Au-μPAD, with CeO_2 immobilized via single-strand hybridization, leveraging their synergistic catalysis of H_2O_2 reduction for amplified current signals and high sensitivity. For colorimetric detection, DSN released CeO_2 into a development zone where it oxidized 3,3′,5,5′-tetramethylbenzidine (TMB) with H_2O_2, producing blue bands whose length correlated quantitatively with target concentration. By adding different miRNA sequences, μPAD exhibited corresponding responses only to the target miRNA, indicating excellent selectivity. While dual-nanomaterial catalysis enhanced sensitivity/efficiency over traditional colorimetry, visual band-length measurement remains susceptible to operator variability and environmental factors (light/angle), limiting precision. Furthermore, a strategy which reduces total turnaround rime, sample volume and cost was developed for the first time to achieve ultra-sensitive, high specificity, rapid quantification and monitoring of cardiac troponin-I antigen (cTnI) and miR-499-5p in untreated saliva, urine and interstitial fluid (ISF) [77]. In this method, AuNPs enhanced $Ru(bpy)_3^{2+}$ electrochemiluminescence (ECL) signal by SPR effect. In 123 clinical serum samples, the sensitivity and specificity of POCT equipment for detecting cTnI were 100 % and 98 %, respectively. In 55 clinical serum samples, the sensitivity of miR-499-5p was 100 % and the specificity was 97 %.

Chattraitat et al. [83] developed a ZnO nanowire-based thermofluidic device for rapid separation of extracellular vesicles (EV-bound) and EV-free miRNAs in serum. Unlike conventional methods, it uses hydrogen bonding to capture both targets simultaneously on nanowires, then exploits thermal stability differences to release free miRNAs while EVs remain intact. It requires 35 min and only 50 μL sample without pretreatment. Compared with traditional EV capture methods requiring specific EV markers, the novel method does not require specific markers and can capture the entire EV and non-EV miRNA, which greatly shortens the time for specific detection. However, the downstream analysis still relies on qPCR/sequencing, limiting on-site use. Portable chip systems can be developed by integrating in-situ detection modules (e.g., electrochemical/optical sensors) with machine learning to analyze multi-source miRNA data.

The CRISPR-Cas system, with its inherent advantages in nucleic acid detection, offers new possibilities for integrating with microfluidic to advance miRNA analysis. With the continuous integration of multiple fields, several teams have attempted to combine the CRISPR-Cas system with microfluidic technology, achieving notable results. Bruch et al. [84] constructed an electrochemical microfluidic platform based on

CRISPR/Cas13a, which can effectively address the limitations such as complex equipment requirements and need for nucleic acid amplification (Fig. 4a (iii)). Experiments using human serum samples demonstrated that this platform could detect potential tumor markers miRNA-19b and miRNA-20a with a LOD at pM level, providing a new technical tool for clinical diagnosis. To address the limitation of insufficient multi-target detection, this same team [76] further divided the microfluidic channel into multiple sub-regions, enabling simultaneous, amplification-free quantitative detection of up to 8 miRNAs simultaneously on one device. However, this multiplexing approach introduces new challenges, including increased complexity in chip fabrication, assay preparation, and readout interpretation. Future efforts could focus on optimizing chip manufacturing, developing standardized readout protocols, and conducting clinical validation.

Beyond single-biomarker detection, Xu et al. [85] focused on simultaneous detection of different types of biomarkers. The team proposed a digital dual CRISPR-Cas-driven single EV evaluation system for highly sensitive and concurrent detection of proteins and miRNAs in single EVs, effectively addressing the specificity challenge of blood-derived EVs. Experiments on plasma samples from breast cancer patients and health donors showed that by evaluating the co-occurrence of PD-L1 protein and miRNA-21, a diagnostic accuracy of 92 % was achieved in distinguishing breast cancer samples from healthy ones. Compared to existing single-EV analysis methods, this system offers higher accuracy in quantifying EV subpopulations concentration. And the use of liposome fusion for miRNAs detection in EVs minimizes contamination from free circulating miRNAs. Additionally, the system enables simultaneous detection of proteins and miRNAs in individual EVs. Therefore, this research is highly promising for advancing EV research and application in disease diagnosis.

By manipulating fluids at a microscale, microfluidics offers advantages such as minimal sample consumption, rapid analysis, high integration, and portability. Its integration with signal amplification, nanomaterials, and CRISPR-Cas system achieves high sensitivity, multi-target, multi-mode detection. The LOD has been continuously reduced with significantly increased detection efficiency. Efforts can be made to optimize the design and manufacturing processes of microfluidic chips to improve their performance and stability. Additionally, conducting clinical trials and strengthening translational research will promote the widespread application in actual medical scenarios.

3.4.2. *Microneedles*

Microneedles (MNs) are arrays composed of dozens of needles, with a height of 50–1500 μM, a tip diameter of 1–100 μM, and a base width of 25–500 μm. MNs penetrate epidermis through their micron-scale array structure to obtain ISF, driven by capillary forces, pump and electroosmotic flow, holding great potential in biomarker detection and therapy. MNs exhibit several advantages including minimal invasiveness, enhanced patient compliance, reduced costs, and real-time monitoring [86]. However, in practical detection, their detection sensitivity is limited by the load capacity of a single needle and signal intensity. Therefore, based on MNs, it is of great significance to achieve highly sensitive miRNA detection by combining signal amplification strategies, nanomaterials, and other strategies.

Signal amplification technology can improve MNs detection performance by enhancing detection signal of targets in animals [87] and plants [88]. Qiao et al. [89] reported a hydrogel microneedle patch integrating GO and gelatin methacryloyl (GelMA) (GO-GelMA) MNs for ISF miRNAs analysis (Fig. 4b (i)). GO-GelMA MNs not only exhibit good mechanical strength to penetrate the stratum corneum (SC) for minimally invasive penetration but also show rapid sampling capability to enrich miRNAs fragments in ISF. Combined with CHA, it enables simultaneous fluorescence detection of 3 psoriasis-specific miRNAs either on patch or in solution. Ex vivo skin model experiments showed that the MNs patch could collect up to 21.34 μL ISF within 30 min, with a LOD at pM level. However, its ability to detect low-abundance miRNAs needs to be further improved, which may lead to missed detections and affect the early diagnosis of diseases. Beyond single-marker detection, a dual-network MN sensor array CHA and carbon quantum dots (CQDs) was constructed to enable simultaneous detection of miRNAs and Cu^{2+} [90]. This method exhibits excellent specificity towards Cu^{2+} and target miRNA, while remaining non-responsive to other metal ions and miRNAs.

Besides CHA strategy, cascade amplification strategies have also been applied in MNs arrays for highly sensitive detection in MNs encapsulated with an intelligent DNA circuit [87]. miRNAs can trigger cascade toehold-mediated DNA displacement reactions, catalytically cleaving cross-linking points and generating amplified fluorescent signals with LOD achieved amazingly at fM level within 5 min.

Integrating nanomaterials (e.g., AgNCs [91], gold-silver nanoparticles (Au-AgNPs) [92]) into MNs systems can significantly enhance detection sensitivity and efficiency, expanding functional capabilities of MNs (Fig. 4b (ii)). Huang et al. [91] combined DNA-templated AgNCs and DSN-mediated signal amplification with porous MNs (Fig. 4b (iii)). miRNAs binding to AgNCs induces fluorescence quenching, while DSN-mediated target recycling further amplifies signal reduction, providing a novel method for detecting cell-free biomarkers with high detection sensitivity. Beyond metal nanoparticles, GO have also been used in MNs arrays, acting as both fluorescence quencher and DNA probe immobilization medium [93,94]. All these methods significantly reduced the fluorescence response of non-complementary miRNA targets and single nucleotide mismatch targets, showing good specificity.

In addition to fluorescence sensing, MN-based electrochemical sensors were developed for miRNA detection [92]. Au-AgNPs modified borosilicate glass microneedle electrodes were developed for detecting miRNA-21-5p after spinal cord injury. In the presence of target, the hairpin DNA specifically recognized target miRNA through base complementary pairing. After miRNA-21-5p binding specifically, electrochemical signal detection was performed and a LOD of 0.3667 fM was achieved in rat spinal cord injury models.

The minimally invasiveness, high sensitivity, good sampling capability, and real-time detection render MNs expandable as a theragnostic platform which can address the limitations of traditional drug administration including high invasiveness, difficulty in self-administration and uneven drug delivery [95,96]. MNs loaded with specific miRNAs can be applied in the treatment of skin diseases, such as alopecia [97], and hypertrophic scars [98]. Chen et al. [99] designed a conductive MN patch combined with zeolitic imidazolate framework-8 (ZIF-8) for targeted and sustained delivery of miRNA-30d to treat myocardial ischemia-reperfusion injury (MIRI). In mouse MIRI models, MNs patch improved left ventricular ejection fraction (LVEF) and fractional shortening (FS). The thread-structural microneedle (T-MN) with unique thread structure can better adapt to mechanical properties of the annulus fibrosus (AF), making them a promising approach for treating intervertebral disc degeneration (IVDD) [100]. It is necessary to establish large animal models with longer follow-up times to verify the applicability of this system.

Despite their promise, MNs face challenges such as limited loading capacity and low sensitivity for detecting low-abundance biomarkers. Their use remains largely confined to research, with clinical translation hindered by issues like standardization, long-term stability, and safety evaluation. Future efforts should focus on developing advanced MN materials (e.g., nanoporous structures) to enhance sensitivity, improving stability and biocompatibility, and conducting clinical trials to validate efficacy across various disease models.

3.4.3. *Other biosensors*

Advanced sensors are the key to achieving trace miRNA detection in complex samples. Other types of biosensors have also been extensively explored, including field-effect transistor (FET) biosensors [101], nanopore sensors [102,103], DNA-PAINT super-resolution microscopy biosensors [104] (Fig. 4c (i)), etc. These biosensors exhibit the

advantages of simple sample processing, high sensitivity, strong specificity, and multi-marker detection with LOD reaching fM or even aM level, which can be employed to detect cancer-related small extracellular vesicles (sEV)-miRNA1246 [105], miRNA-19b-3p [106] and let-7a [107], etc.

Solution-gated graphene transistors (SGGTs) with excellent biocompatibility, chemical stability, high carrier mobility and low operating voltage (<1 V), have been employed in various biosensors. Deng et al. [108] developed an SGGT-based biosensor for detection miRNA-21 by modifying gold gate electrode with ssDNA probes. The sensing mechanism relies on the shift in transfer curves caused by hybridization between the ssDNA probes and target miRNAs. When target concentration is not higher than 10–16 M, the detection time is about 5 min, with a LOD at the aM level. Notably, it can well distinguish one-mismatched miRNA-21 molecule and can directly analyze clinical serum samples from prostate cancer patients and healthy individuals without requiring RNAs extraction, labeling, or polymerase chain reaction (PCR) amplification.

Inspired by single-nanomaterial biosensors, dual nanomaterial integration enhances sensor performance through synergistic effects. A multiplexed electrochemical array sensor was developed for simultaneously detecting four lung cancer-related miRNAs (miRNA-21, miRNA-155, miRNA-205, and let-7b) with a detection limit as low as 92 ± 0.1 aM [109] (Fig. 4c (ii)). Despite promising results from limited clinical samples (7 patients, 1 control), broader studies with diverse patient groups are needed to validate accuracy and clinical applicability.

In recent years, WaveFlex biosensor (refers to fiber optical biosensor), have gained popularity among researchers due to their high biocompatibility and anti-electromagnetic interference capability. Currently, WaveFlex biosensors have been developed for the detection of biomarkers such as aflatoxin [111], des-γ-carboxy prothrombin [112] and miRNA [113]. A novel dual-mode DNA walker fiber optic biosensor for detecting miRNA-155 and miRNA-21 has been proposed [113]. In addition, WaveFlex biosensor is also used for RNA detection in plant [114]. In a wide linear range of 1 pM–100 nM, the LOD of the sensor reaches 0.015 pM. The results show that the LOD can reach 0.015 pM with a wide linear range of 1 pM–100 nM.

To solve the problems of optical sensor detection limit and background interference, Hui et al. [115] constructed a plasma biosensor based on surface-enhanced infrared absorption (SEIRA) using metamaterial perfect absorber (MPA) and tetrahedral DNA nanostructure (TDN). The Fabry-Perot optical cavity formed by the MPA can provide near-field intensity enhancement up to 1000 times higher than the fingerprint spectral band of miRNA-155. TDNs served as probes, exhibiting 5000 times higher affinity than single-stranded DNA probes and 100 times lower LOD than fluorescence methods. The LOD for miRNA-155 is as low as 100 fM. A similar result was achieved by Springer group [116]. They developed a SPR biosensor based on oligonucleotide-triggered release of AuNPs from the surface to detect miRNA-125b and miRNA-16 in myelodysplastic syndrome. Plasma results from patients with human myelodysplastic syndrome showed that the LODs of miRNA-125b and miRNA-16 were 349 aM and 550 aM, respectively. In terms of real-time monitoring, Wang et al. [117] proposed a polydisperse droplet digital CRISPR/Cas13a (PddCas13a) biosensor. Once activated, Cas13a can non-specifically cleave RNAs, and the reaction can be monitored in real-time through fluorescent signals without polymerase-based amplification and LOD reaching as low as approximately 10 aM.

Furthermore, other research teams have improved detection performance by developing various types of biosensors, including: an electrochemical sensor combining silver nanoparticles with strand displacement amplification and CHA [110] (Fig. 4c (iii)), a SERS-colorimetric dual-mode biosensor integrating Fe_3O_4@$mSiO_2$ with primer exchange reaction [118], and a self-powered biosensor based on ultrathin graphdiyne combined with nucleic acid amplification [119]. These biosensors achieve LODs as low as fM or even aM level and exhibit good specificity, providing effective methods for various miRNAs detection.

3.5. Enhanced miRNA detection facilitated by AI

AI is overwhelmingly being applied in developing novel miRNA detection strategies, including paper-based biosensors [120], lateral flow assays (LFAs) [121], and nanomaterials-driven methods [122]. The unique advantages of AI include its capacity for deep feature extraction to distinguish true signals from background noise, and the incorporation of high-dimensional feature learning to classify similar signals. This effectively enhances data quality, greatly reduces reliance on high-precision instrumentation, and substantially overcomes the detection limits of conventional methods [123]. Therefore, it is widely utilized to predict miRNA structure and functional associations in diseases [124], accurately quantify in complex samples [125], optimize signal extraction efficiency [126], and improve signal-to-noise ratio (SNR) [127].

Marked by explosive growth in AI technology, several studies have focused on integrating AI into traditional miRNA detection methods for effectively amplifying miRNA signals. For instance, Ma et al. [128] developed an AI-based signal amplification (AISA) system for sensitive detection of miRNAs in vitro and in vivo. This system comprises double-stranded SQ (where S represents the signal strand and Q the quencher strand) and FP (where F is the fuel strand and P the guard strand). Within the AISA framework, the AI selects an optimal parameter set from a broad range by analyzing the SNR across variables such as dangling strand length and the SQ/FP ratio. Furthermore, by learning from training data on fluorescence intensity, tissue depth, and actual concentration, the AI constructs a calibration model to correct for quantitative bias induced by signal attenuation, thereby significantly enhancing detection accuracy. While most prior strategies amplified miRNA signals in vitro, this approach innovatively achieves in vivo amplification of miRNA-derived signals and enables their direct visualization.

AI is also widely used to assist in the measurement process of LFA system. LFAs offer advantages such as rapid detection, simple operation, easy production, suitable for POCT cost-effectiveness [129]. However, traditional LFA systems suffer from drawbacks such as low sensitivity, weak ability to distinguish low-concentration samples, and poor quantification capabilities. To address these shortcomings, Wang et al. [130] designed a dual-nanomaterial LFA detection method, using gold nanoparticles (AuNPs) to enhance the fluorescence signal of fluorescent nanodiamonds (FNDs). In turn, FNDs enhance the color intensity of GNPs, forming a synergistic effect of mutual enhancement between fluorescence and color development. Then, through vector regression (SVR) and Gaussian process regression (GPR) algorithms, the visual chromatographic signal and fluorescence spectral signal were convolved, fused, and synergistically analyzed, which effectively amplified the weak signal of low-concentration miRNA, making the LOD reach the fM level, which is far superior to the pM level of traditional LFAs. Moreover, by integrating a dual lightweight convolutional neural network (CNN) model (YOLO v5 and MobileNet v3) into CRISPR-mediated lateral flow assays (CLFAs), AI enables ultrasensitive, one-step detection of cervical cancer biomarker miRNA-21 with a detection limitation of 38 aM, achieving precise quantification through automated test line localization and feature-based concentration regression [131].

Furthermore, machine learning algorithms can also be applied to analyze complex miRNA data in SERS, enabling effective target identification, complex spectral interpretation, and quantitative detection [132]. The random forest (RF) algorithm can enhance the detection efficiency of sensors for dual-target, which is specifically reflected in accurate classification and differentiation of targets, improved quantitative accuracy in the low-concentration range, and increased data analysis efficiency [133].

In summary, the incorporation of AI into miRNA detection methodologies significantly improves signal amplification, increases sensitivity, and allows for precise quantification within complex samples matrices. AI effectively addresses numerous constraints of conventional techniques, heralding a new era for its application as a powerful tool in advanced data analysis, spectral interpretation, and tracking disease progression.

4. Enhancement mechanism and selective recognition

Table 1 summarizes a variety of miRNA detection methods, each centered around enhancing signal intensity or detection efficiency through specific amplification mechanisms to achieve high sensitivity, specificity, and selectivity, briefly introduced below.

4.1. Enhancement mechanism

4.1.1. Enhanced cascade efficiency

Enhanced cascade efficiency improves signal amplification efficiency by integrating multiple rounds of nucleic acid amplification reactions (such as CHA, RCA, HCR, etc.), optimizing reaction kinetics, and reducing invalid consumption. It is one of the core strategies for miRNA detection (Table 1, refs [31,82]).

This cascade technique can achieve exponential amplification. Moreover, multiple rounds of target recognition allow for efficient selection of target miRNA, improve the selectivity for highly homologous sequences of miRNA family members, and reduce cross-interference [134,135]. However, the practicality of this method can be hindered by drawbacks such as complex reaction steps, lengthy duration, and enzyme dependence [136].

4.1.2. Confined space enrichment

The confinement of molecules within nano- or micro-scale regions enables the enrichment of targets by altering molecular motion and reaction kinetics, which significantly enhances local concentration while reducing external signal interference. By confining signal molecules in confined spaces (e.g., hydrogels, microneedles) or microchannels, local molecular concentration and binding sites are increased, accelerating amplification, and enabling efficient signal enrichment, typically in RCA, MNs, and microfluidic systems (Table 1, refs [24,75,87,88]).

This strategy offers several key benefits for miRNA detection [137,138]. It can physically isolate complex environmental interference and increase local target molecule concentration, thus accelerating the reaction kinetics by shortening molecular diffusion distance. However, this approach faces practical challenges. The assembly and purification of the nanomaterials that create these spaces can be complex, and their limited capacity can lead to signal saturation at high target concentration [139].

4.1.3. Field enhancement

Field enhancement forms a strong electromagnetic field in local regions by regulating the interaction between nanostructures and light to amplify the optical signals of target molecules. Taking metal nanoparticles (e.g., Au/Ag) as examples, they leverage LSPR to generate field enhancement effects, achieving signal amplification with target miRNA binding (Table 1, refs [51,52]).

The application of field enhancement overcomes the limitations of traditional optical detection, enabling label-free detection. Furthermore, it maintains stability and repeatability in complex detection scenarios such as body fluids and cells, which greatly improves detection sensitivity [140].

4.1.4. QDs confinement effect

By regulating the size and structure of QDs, the QDs confinement effect restricts electrons and holes within a 3D space. This creates a discrete energy level structure allowing QDs to produce narrow-band and high-intensity fluorescence (Table 1, ref [45]).

In resonance energy transfer systems, the QDs confinement effect can enhance energy transfer efficiency, reduce background interference, and improve the signal-to-noise ratio [141,142]. The viability of this strategy is challenged by concerns regarding heavy metal release, oxidative damage, and costly synthesis processes [143].

4.1.5. Improved charge transfer

Improved charge transfer can improve the efficiency of electron/charge transfer in biosensing systems by optimizing the interface structure of materials or introducing functionalized molecules. For instance, the unique electrical properties of nanomaterials can significantly enhance electron transport efficiency, improve interface performance, and regulate carrier dynamics. These effects amplify detection signals and improve sensitivity (Table 1, ref [51]).

The improvement of charge transfer efficiency can directly enhance the signal response strength, thus the LOD can reach as low as fM or even aM level. However, the detection instruments based on this mechanism mostly rely on precise material structure and their preparation processes are relatively complex [144].

In general, the enhancement principles for highly sensitive miRNA detection are diverse and can be used synergistically. These strategies significantly improve detection sensitivity and specificity through various approaches, including physical space confinement, reaction kinetics optimization, multi-level signal synergistic amplification, and leveraging the unique characteristics of nanomaterials. They provide strong technical support for the application of miRNA in disease diagnosis and treatment monitoring.

4.2. Selective recognition mechanism

4.2.1. Probe structure design

Nucleic acid probes serve as the core components for recognizing miRNA and their structural design plays a pivotal role in optimizing recognition performance, as it pre-ensures the spatial conformation of the probe, which directly determines its binding affinity, specificity, and signal generation efficiency. Currently, A variety of probe structures are widely employed, including hairpin structure [145], stem-loop structure [146], double-stranded structure [147], polyhedral structure [148]. For instance, the design of dumbbell-shaped probes introduces a novel recognition strategy. Only when the target miRNA binds to the bases of the toehold domain of the sealed probe and the strand displacement reaction causes the sealed probe to switch from a dumbbell shape to an “activated” circle, will RCA be activated. Due to the resistance of the stable dumbbell structure, mismatched miRNAs cannot induce such structural transition and thus no amplification will occur [149].

4.2.2. Probe length design

To precisely select target miRNAs, probes are primarily designed with a moderate length. Excessively short or long probes are unfavorable to target binding. Since the binding between a probe and target relies on base stacking forces, short probes lack sufficient base pairs, leading to unstable binding. While, overly long probes form too many base pairs, resulting in relatively strong binding force. In this case, miRNA with a single-base mismatch only have limited disruption to the overall stability and cannot be distinguished [150]. Therefore, A moderate length can provide sufficient binding sites for target miRNA and reduce the stability of hybrids with mismatched miRNA. For example, optimizing crRNA (the probe) length in the CRISPR-Cas13a system improve single-nucleotide mismatch discrimination. When comparing three spacer lengths (28 nt, 20 nt, and 16 nt), the 28 nt spacer tolerates mismatches at high target concentration and activates Cas13a. In contrast, when using the 20 nt spacer, only perfectly matched target RNA can efficiently activate Cas13a at low target concentration. Although the 16 nt spacer exhibits the highest mismatch sensitivity, it severely reduces

Table 1
Strategies and mechanisms for highly sensitive detection of miRNA.

Method		Mechanism		LOD	Detection range	Test sample	Ref.
Signal amplification	RCA	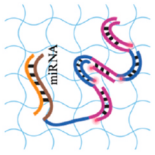	confined space effect	46 aM	low zmol-tens of amol	serum sample	[24]
	CHA	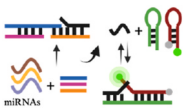	enhanced cascade efficiency	miR-133a: 32.86 pM miR-499: 17.71 pM miR-21: 22.48 pM	0.05–20 nM	serum sample mouse tissue	[31]
		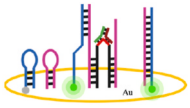	dual signal amplification	10 aM	100 aM-0.1 pM	cell human tissue sample	[32]
	HCR	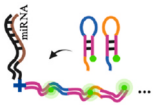	multiplex signal amplification	miR-6090: 1–10 amol miR-3665: 10–100 amol	0.02–20 pM	urine specimen	[35]
Nano	QD	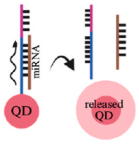	quantum confinement effect	miR-155: 7.19 fM miR-150: 5.84 fM	10 fM-1 nM	serum sample	[45]
	ZnO	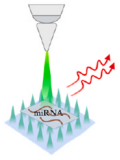	improved charge transfer	1 μM	1 μM–100 μM	buffer solution	[51]
	Au + Ag	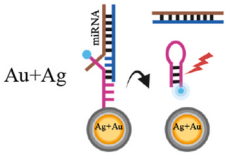	field enhancement	miR-21: 6.8 zmol miR-221: 16.7 zmol	–	serum sample	[52]
CRISPR-Cas		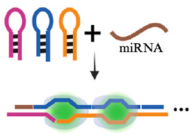	multiplex signal amplification	1 fM	1 fM-100 nM	cell	[65]
		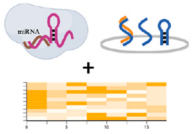	Multiplex signal amplification + machine learning	8.26 fM	10 fM-10 nM	plasma sample	[69]
Other devices	Microfluidic	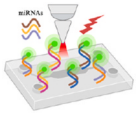	increased binding site and enrichment	0.146 aM	1 aM-10 nM	serum sample	[75]
		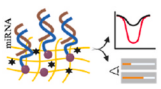	nano catalysis + cascade amplification	electrochemical: 0.12 fM visual: 2.65 fM	electrochemical: 10 fM-1 nM visual: 0.5 fM-1 nM	buffer solution	[82]

(*continued on next page*)

Table 1 (*continued*)

Method	Mechanism		LOD	Detection range	Test sample	Ref.
	Microneedle	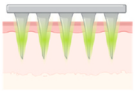	confined enrichment	241.56 pM	10 fM-200 nM cell living animal	[87]
		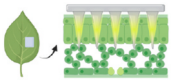	confined space enrichment	89 pM	0.2 nM–100 nM	plant leaves	[88]
	Biosensor	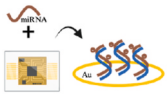	improved electronic mobility	0.01 aM	0.01 aM-1 pM	serum sample	[108]
		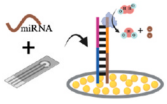	enrichment and catalytic amplification	92 aM	100 aM-10 pM	cell serum sample	[109]

the overall cleavage and detection efficiency [151].

4.2.3. Interaction enhancement

Specific modification and optimization of the recognition probe enable a significant boost in binding affinity toward the target miRNA, consequently improving selectivity for the intended sequence. These forces include hydrogen bonds [152], van der Waals forces [153], electrostatic interactions [154] and other intermolecular forces. For example, a moderate probe length ensures the formation of a sufficient number of hydrogen bonds with target miRNA to guarantee binding stability, while also allowing irrelevant sequences with single-base mismatches to be denatured at low-temperature [155]. In addition, Li et al. [154] successfully developed a low-background ECL biosensor for miRNA detection by modulating the electrostatic properties of the probes and their immobilized interface. By leveraging the difference in electrostatic attraction between the positively charged indium tin oxide (ITO) electrode interface and the negatively charged $Ru(phen)_2^{3+}$-dsDNA complex, this sensor effectively shielded against non-target miRNAs.

5. Conclusions and perspective

This article reviews recent advances in miRNA detection methods over the past five years, highlighting innovations in signal amplification, nanomaterials, CRISPR-Cas systems, biosensors, and integrated technologies. While these approaches have greatly improved sensitivity, specificity, and efficiency, several limitations remain to be addressed.

From the perspective of detection capability, current methods struggle to simultaneously meet key indicators, including high sensitivity, specificity, multiplexing capacity, and rapid detection. For example, nanomaterials can lower the LOD by over 2000-fold compared to traditional techniques, but they are mainly limited to single biomarker detection, resulting in low detection throughput. From the perspective of clinical transformation, most techniques remain at the laboratory stage, with few applied in clinical practice. This is due to (1) lack of standardization in different methods may yield inconsistent results when analyzing the same miRNAs sample; (2) high costs-techniques relying on nanomaterials or CRISPR-Cas systems involve expensive instrumentation, hindering large-scale clinical adoption.

The continuous development of signal amplification technology promotes primers design optimization and reaction conditions to enhance signal amplification efficiency and reduce background noise. In the field of nanomaterials, developing novel materials and fabrication techniques enable large-scale and low-cost production. For CRISPR-Cas systems, further modification and optimization of Cas proteins can overcome current problems such as PAM restrictions and off-target effects, expanding application scenarios. Furthermore, biosensors can focus on developing new recognition elements and signal transduction mechanisms to improve detection accuracy and enhance adaptability to complex samples. Additionally, integrating with multiple technologies can become a key direction in future research.

AI has demonstrated excellent properties in optimizing signal amplification, improving sensitivity, and accurate quantification. AI facilitates complex data analysis, and improves diagnostic capabilities in POCT, making it a crucial component in miRNA detection through effectively overcoming low sensitivity and poor SNR and enabling detection to be applied with higher performance and reliability in clinical practice.

CRediT authorship contribution statement

Yuhan Wang: Writing – original draft. **Zijian Liu:** Writing – original draft. **Hen-Wei Huang:** Writing – review & editing. **Jung Seung Lee:** Writing – review & editing. **Kexin Liu:** Formal analysis. **Mengru Yu:** Formal analysis. **Xiaoyue Qi:** Writing – review & editing, Supervision, Funding acquisition, Conceptualization.

Declaration of competing interest

The authors declare that they have no known competing financial interests or personal relationships that could have appeared to influence the work reported in this paper.

Acknowledgments

This work is financially supported by the Beijing Natural Science Foundation (No.52004020), National Natural Science Foundation of China (No. 22404004), Hebei Natural Science Foundation (No. C2025105024), Beijing Key Laboratory of Mental Disorders (No. 2023JSJB01), the Foundation of the State Key Laboratory of Transducer Technology (No. SKT2308), and the open funds of the State Key Laboratory of Chemo and Biosensing (Hunan University, (2025)0937-8).

Data availability

No data was used for the research described in the article.

References

[1] X. Meng, X. Pang, J. Yang, X. Zhang, H. Dong, Small 20 (2024) 2307701.
[2] Z. Zhang, T. Liu, M. Dong, M.A. Ahamed, W. Guan, WIREs nanome, Nanobiotechnol 16 (2024) e1969.

[3] E.M. Small, R.J.A. Frost, E.N. Olson, Circulation 121 (2010) 1022.
[4] C. Fernández-Hernando, C.M. Ramírez, L. Goedeke, Y. Suárez, Thromb Arteriosclerosis, Vasc. Biol. 33 (2013) 178.
[5] J. Wang, Y. Cao, X. Lu, T. Wang, S. Li, X. Kong, C. Bo, J. Li, X. Wang, H. Ma, L. Li, H. Zhang, S. Ning, L. Wang, Brief. Bioinform. 21 (2019) 863.
[6] D. Mukhopadhyay, C. P, O. S, C. R, S. De Matteis, Pulmonology 31 (2025) 2416792.
[7] K. Zhao, Z. Li, L. Zeng, Z. Cai, R. Liu, Front. Immunol. 15 (2024), 2024.
[8] T. Fehlmann, B. Lehallier, N. Schaum, O. Hahn, M. Kahraman, Y. Li, N. Grammes, L. Geffers, C. Backes, R. Balling, F. Kern, R. Krüger, F. Lammert, N. Ludwig, B. Meder, B. Fromm, W. Maetzler, D. Berg, K. Brockmann, C. Deuschle, A.-K. von Thaler, G.W. Eschweiler, S. Milman, N. Barziliai, M. Reichert, T. Wyss-Coray, E. Meese, A. Keller, Nat. Commun. 11 (2020) 5958.
[9] L. Gorgani, M. Mohammadi, G. Najafpour Darzi, J.B. Raoof, Talanta 273 (2024) 125854.
[10] N.B. Aziz, R.G. Mahmudunnabi, M. Umer, S. Sharma, M.A. Rashid, Y. Alhamhoom, Y.-B. Shim, C. Salomon, M.J.A. Shiddiky, Analyst 145 (2020) 2038.
[11] T. Ouyang, Z. Liu, Z. Han, Q. Ge, Anal. Chem. 91 (2019) 3179.
[12] J. Ye, M. Xu, X. Tian, S. Cai, S. Zeng, J. Pharm. Anal. 9 (2019) 217.
[13] J. Yang, J. Chen, L. Xia, G. Li, Talanta 294 (2025) 128219.
[14] P. Khashayar, S. Al-Madhagi, M. Azimzadeh, V. Scognamiglio, F. Arduini, TrAC Trends Anal. Chem. 156 (2022) 116706.
[15] X. Lu, C. Yao, L. Sun, Z. Li, Biosens. Bioelectron. 203 (2022) 114041.
[16] N. Wang, J. Zhang, B. Xiao, X. Sun, R. Xie, A. Chen, Biosens. Bioelectron. 211 (2022) 114345.
[17] G. Moro, C.D. Fratte, N. Normanno, F. Polo, S. Cinti, Angew. Chem. 135 (2023) e202309135.
[18] M. Negahdary, L. Angnes, Coord. Chem. Rev. 464 (2022) 214565.
[19] T. Jet, G. Gines, Y. Rondelez, V. Taly, Chem. Soc. Rev. 50 (2021) 4141.
[20] M.G. Dastidar, U. Schumann, D.R. Nisbet, R. Natoli, K. Murugappan, A. Tricoli, Chem. Eng. J. 508 (2025) 160903.
[21] C. Song, W. Chen, J. Kuang, Y. Yao, S. Tang, Z. Zhao, X. Guo, W. Shen, H.K. Lee, TrAC Trends Anal. Chem. 139 (2021) 116269.
[22] S. Yue, Y. Li, Z. Qiao, W. Song, S. Bi, Trends Biotechnol. 39 (2021) 1160.
[23] J. Liu, G. Xie, S. Lv, Q. Xiong, H. Xu, TrAC Trends Anal. Chem. 160 (2023) 116953.
[24] D. Al Sulaiman, N. Juthani, P.S. Doyle, Adv. Healthc. Mater. 11 (2022) 2102332.
[25] C.-C. Wu, K.-T. Hsieh, S.-Y. Yeh, Y.-T. Lu, L.-J. Chen, M.S.B. Ku, W.-H. Li, Plant Biotechnol. J. 21 (2023) 136.
[26] S. Jiang, Q. Liu, J. Hu, D. Yuan, Y. Zhang, C.-y. Zhang, Sens. Actuators B: Chem. 373 (2022) 132689.
[27] C.-C. Li, J. Hu, X. Zou, X. Luo, C.-Y. Zhang, Anal. Chem. 94 (2022) 1882.
[28] Z. Jiao, N.-n. Zhao, S.-h. Wei, D.-l. Li, T. Wang, C.-y. Zhang, Sens. Actuators B: Chem. 433 (2025) 137542.
[29] L. Zhao, Y. Song, H. Xu, TrAC, Trends Anal. Chem. 171 (2024) 117508.
[30] Y. Wu, C. Fu, W. Shi, J. Chen, Talanta 235 (2021) 122735.
[31] C. Yang, H. Ou, Y. Zhao, L. Mo, W. Lin, Sens. Actuators B: Chem. 417 (2024) 136063.
[32] P. Miao, Y. Tang, ACS Cent. Sci. 7 (2021) 1036.
[33] Z.W. Wong, S.Y. New, Small Methods 9 (2025) 2401436.
[34] K. Morihiro, Y. Tomida, D. Fukui, M. Hasegawa, A. Okamoto, Angew. Chem. Int. Ed. 62 (2023) e202306587.
[35] J. Kim, J.S. Shim, B.H. Han, H.J. Kim, J. Park, I.-J. Cho, S.G. Kang, J.Y. Kang, K. W. Bong, N. Choi, Biosens. Bioelectron. 192 (2021) 113504.
[36] L.-j. Wang, M. Ren, H.-x. Wang, J.-G. Qiu, B. Jiang, C.-y. Zhang, Anal. Chem. 92 (2020) 8546.
[37] J. Lim, J.-S. Hwang, S. Beom Seo, B. Kang, S. Jang, S. Uk Son, J. Ki, J.-S. Kim, T. Kang, J. Jung, T.-S. Han, E.-K. Lim, Chem. Eng. J. 448 (2022) 137637.
[38] X. Wang, S. Shepherd, N. Li, C. Che, T. Song, Y. Xiong, I.R. Palm, B. Zhao, M. Kohli, U. Demirci, Y. Lu, B.T. Cunningham, Angew. Chem. Int. Ed. 62 (2023) e202217932.
[39] Y. Lei, X. Fei, Y. Ding, J. Zhang, G. Zhang, L. Dong, J. Song, Y. Zhuo, W. Xue, P. Zhang, C. Yang, Sci. Adv. 9 (2023) eadi1556.
[40] M. Yang, L. Zhu, W. Yang, W. Xu, Coord. Chemi. Rev. 491 (2023) 215247.
[41] H.C. Yadavalli, S. Park, Y. Kim, R. Nagda, T.-H. Kim, M.K. Han, I.L. Jung, Y. J. Bhang, W.H. Yang, L.T. Dalgaard, S.W. Yang, P. Shah, Small 20 (2024) 2306793.
[42] A. Robles-Remacho, I. Martos-Jamai, M. Tabraue-Chávez, A. Aguilar-González, J. A. Laz-Ruiz, M.V. Cano-Cortés, F.J. López-Delgado, J.J. Guardia-Monteagudo, S. Pernagallo, J.J. Diaz-Mochon, R.M. Sanchez-Martin, J. Nanobiotechnol. 22 (2024) 791.
[43] Q. Xu, J. Gao, S. Wang, Y. Wang, D. Liu, J. Wang, J. Mater. Chem. B 9 (2021) 5765.
[44] Z. Yu, Y. Zheng, H. Cai, S. Li, G. Liu, W. Kou, C. Yang, S. Cao, L. Chen, X. Liu, Z. Wan, N. Zhang, X. Li, G. Cui, Y. Chang, Y. Huang, H. Lv, T. Feng, Sci. Adv. 10 (2024) eadl6442.
[45] J.J. Wang, Y. Liu, Z. Ding, L. Zhang, C. Han, C. Yan, E. Amador, L. Yuan, Y. Wu, C. Song, Y. Liu, W. Chen, Bioact. Mater. 17 (2022) 360.
[46] F. Ma, Q. Zhang, C.-y. Zhang, Nano Lett. 19 (2019) 6370.
[47] Y. Xiong, Q. Huang, T.D. Canady, P. Barya, S. Liu, O.H. Arogundade, C.M. Race, C. Che, X. Wang, L. Zhou, X. Wang, M. Kohli, A.M. Smith, B.T. Cunningham, Nat. Commun. 13 (2022) 4647.
[48] P. Zhang, Y. Ouyang, Y.S. Sohn, M. Fadeev, O. Karmi, R. Nechushtai, I. Stein, E. Pikarsky, I. Willner, ACS Nano 16 (2022) 1791.
[49] J. Wang, S. Ma, K. Ge, R. Xu, F. Shen, X. Gao, Y. Yao, Y. Chen, Y. Chen, F. Gao, G. Wu, Anal. Chem. 96 (2024) 8922.
[50] H.-S. Su, X. Chang, B. Xu, Chi. J. Catal. 43 (2022) 2757.
[51] Z. Wu, D. Zhao, X. Han, J. Liu, Y. Sun, Y. Li, Y. Duan, J. Nanobiotechnol. 21 (2023) 17.
[52] A.J. Canning, X. Chen, J.Q. Li, W.R. Jeck, H.-N. Wang, T. Vo-Dinh, Biosens. Bioelectron. 220 (2023) 114855.
[53] H.V. Tran, B. Piro, Microchim. Acta 188 (2021) 128.
[54] A. Taghavi-Kahagh, F. Behboodi-Sadabad, M. Salami-Kalajahi, J. Mater. Chem. B 13 (2025) 7226.
[55] L. Velmanickam, D. Nawarathna, Front. Lab Chip Technol. 3 (2024), 2024.
[56] S. Qureshi, S. Anjum, M. Hussain, A. Sheikh, G. Gupta, M.A.A. Almoyad, S. Wahab, P. Kesharwani, Int. J. Pharm. 660 (2024) 124301.
[57] R. Ren, M. Sun, P. Goel, S. Cai, N.A. Kotov, H. Kuang, C. Xu, A.P. Ivanov, J. B. Edel, Adv. Mater. 33 (2021) 2103067.
[58] B. Cai, Z. Xia, J. Wang, S. Wu, X. Jin, ACS Applied Nano Mater 5 (2022) 12035.
[59] D.S. Sharma, P.H.S. Siddharth, A. Fayaz, S. Patil, D. Rath, Talanta 298 (2025) 128891.
[60] D.S. Sharma, P.H.S. Siddharth, A. Fayaz, S. Patil, D. Rath, Talanta 298 (2025) 128891.
[61] L. Zhao, X. Deng, Y. Li, Q. Zhao, L. Xiao, J. Xue, A. Chen, W. Cheng, M. Zhao, J. Nanobiotechnol. 22 (2024) 684.
[62] J.-S. Hong, T. Son, C.M. Castro, H. Im, Adv. Sci. 10 (2023) 2301766.
[63] T.S. Zavvar, Z. Khoshbin, M. Ramezani, M. Alibolandi, K. Abnous, S.M. Taghdisi, Biosens. Bioelectron. 214 (2022) 114501.
[64] M. Zhong, K. Chen, W. Sun, X. Li, S. Huang, Q. Meng, B. Sun, X. Huang, X. Wang, X. Ma, P. Ma, Biosens. Bioelectron. 214 (2022) 114497.
[65] H.-Y. Jia, H.-L. Zhao, T. Wang, P.-R. Chen, B.-C. Yin, B.-C. Ye, Biosens. Bioelectron. 211 (2022) 114382.
[66] P. Chen, L. Wang, P. Qin, B.-C. Yin, B.-C. Ye, Biosens. Bioelectron. 207 (2022) 114152.
[67] Q. Zhang, Y. Han, C.-c. Li, X. Zou, F. Ma, C.-y. Zhang, Chem. Communi. 58 (2022) 5538.
[68] X. Shen, Z. Lin, X. Jiang, X. Zhu, S. Zeng, S. Cai, H. Liu, Biosens. Bioelectron. 264 (2024) 116676.
[69] J. Pei, L. Li, C. Li, Z. Li, Y. Wu, H. Kuang, P. Ma, L. Huang, J. Liu, G. Tian, Biosens. Bioelectron. 273 (2025) 117190.
[70] H. Yan, Y. Wen, Z. Tian, N. Hart, S. Han, S.J. Hughes, Y. Zeng, Nat. Biomed. Eng. 7 (2023) 1583.
[71] H. Liu, J. Dong, Z. Duan, F. Xia, I. Willner, F. Huang, Sci. Adv. 10 (2024) eadp6166.
[72] C. Wang, X. Xu, W. Yao, L. Wang, X. Pang, S. Xu, X. Luo, Nano Lett. 25 (2025) 1666.
[73] Z. Tong, X. Xu, C. Shen, D. Yang, Y. Li, Q. Li, W. Yang, F. Xu, Z. Wu, L. Zhou, C. Zhan, H. Mao, Biosens. Bioelectron. 270 (2025) 116976.
[74] K. Zhao, Z. Peng, H. Jiang, X. Lv, X. Li, Y. Deng, Sens. Actuators B: Chem. 361 (2022) 131741.
[75] Y. Chu, Y. Gao, W. Tang, L. Qiang, Y. Han, J. Gao, Y. Zhang, H. Liu, L. Han, Anal. Chem. 93 (2021) 5129.
[76] R. Bruch, M. Johnston, A. Kling, T. Mattmüller, J. Baaske, S. Partel, S. Madlener, W. Weber, G.A. Urban, C. Dincer, Biosens. Bioelectron. 177 (2021) 112887.
[77] H. Xiong, C. Zhu, C. Dai, X. Ye, Y. Li, P. Li, S. Yang, G. Ashraf, D. Wei, H. Chen, H. Shen, J. Kong, X. Fang, Adv. Sci. 11 (2024) 2307840.
[78] S. Chen, J. Zhao, I.Y. Sakharov, J. Xu, C. Xu, S. Zhao, Biosens. Bioelectron. 203 (2022) 114053.
[79] J. Qian, Q. Zhang, M. Liu, Y. Wang, M. Lu, Biosens. Bioelectron. 196 (2022) 113707.
[80] Y. Zhao, X. Fang, M. Bai, J. Zhang, H. Yu, F. Chen, Y. Zhao, Chin. Chem. Lett. 33 (2022) 2101.
[81] X. Liu, Y. Wang, Y. Du, J. Zhang, Y. Wang, Y. Xue, J. Zhao, L. Ge, L. Yang, F. Li, Chem. Eng. J. 486 (2024) 150233.
[82] C. Zhou, K. Cui, Y. Liu, L. Li, L. Zhang, S. Hao, S. Ge, J. Yu, ACS Appl. Mater. Interfaces 13 (2021) 32780.
[83] K. Chattrairat, A. Yokoi, M. Zhang, M. Iida, K. Yoshida, M. Kitagawa, A. Niwa, M. Maeki, T. Hasegawa, T. Yokoyama, Y. Tanaka, Y. Miyazaki, W. Shinoda, M. Tokeshi, K. Nagashima, T. Yanagida, H. Kajiyama, Y. Baba, T. Yasui, Device 2 (2024).
[84] R. Bruch, J. Baaske, C. Chatelle, M. Meirich, S. Madlener, W. Weber, C. Dincer, G. A. Urban, Adv. Mater. 31 (2019) 1905311.
[85] X. Xu, Y. Zhang, J. Liu, S. Wei, N. Li, X. Yao, M. Wang, X. Su, G. Jing, J. Xu, Y. Liu, Y. Lu, J. Cheng, Y. Xu, ACS Nano 19 (2025) 1271.
[86] Z. Li, Y. Wang, R. Zhang, Z. Liu, Z. Chang, Y. Deng, X. Qi, ACS Nano 18 (2024) 23876.
[87] Q. Yang, Y. Wang, T. Liu, C. Wu, J. Li, J. Cheng, W. Wei, F. Yang, L. Zhou, Y. Zhang, S. Yang, H. Dong, ACS Nano 16 (2022) 18366.
[88] L. Chen, X. Ding, Y. Dong, H. Chen, F. Gao, B. Cui, X. Zhao, H. Cui, X. Gu, Z. Zeng, Sens. Actuators B: Chem. 404 (2024) 135277.
[89] Y. Qiao, J. Du, R. Ge, H. Lu, C. Wu, J. Li, S. Yang, S. Zada, H. Dong, X. Zhang, Anal. Chem. 94 (2022) 5538.
[90] J. Li, H. Lu, Y. Wang, S. Yang, Y. Zhang, W. Wei, Y. Qiao, W. Dai, R. Ge, H. Dong, Anal. Chem. 94 (2022) 968.
[91] R. Huang, P. Wan, S. Hu, C. Zhang, W. Miao, ACS Sens. 9 (2024) 5604.
[92] C. Wang, C. Wang, M. Wang, M. Wang, Q. Ni, J. Sun, B. Sun, Y. Wang, ACS Sens. 9 (2024) 5058.

[93] F. Keyvani, H. Zheng, M.R. Kaysir, D.F. Mantaila, P. Ghavami Nejad, F. A. Rahman, J. Quadrilatero, D. Ban, M. Poudineh, Angew. Chem. Int. Ed. 62 (2023) e202301624.
[94] H. Zheng, F. Keyvani, S. Sadeghzadeh, D.F. Mantaila, F.A. Rahman, J. Quadrilatero, M. Poudineh, Lab Chip 24 (2024) 4989.
[95] V. Singh, P. Kesharwani, J. Control. Release 338 (2021) 394.
[96] Z. Le, J. Yu, Y.J. Quek, B. Bai, X. Li, Y. Shou, B. Myint, C. Xu, A. Tay, Mater. Today 63 (2023) 137.
[97] Y. Zhao, Y. Tian, W. Ye, X. Wang, Y. Huai, Q. Huang, X. Chu, X. Deng, A. Qian, Biomater. Sci. 11 (2023) 140.
[98] S. Meng, Q. Wei, S. Chen, X. Liu, S. Cui, Q. Huang, Z. Chu, K. Ma, W. Zhang, W. Hu, S. Li, Z. Wang, L. Tian, Z. Zhao, H. Li, X. Fu, C. Zhang, Small 20 (2024) 2305374.
[99] X. Chen, H. Chen, L. Zhu, M. Zeng, T. Wang, C. Su, G. Vulugundam, P. Gokulnath, G. Li, X. Wang, J. Yao, J. Li, D. Cretoiu, Z. Chen, Y. Bei, ACS Nano 18 (2024) 19470.
[100] S. Hu, M. Zhu, H. Xing, Y. Xue, J. Li, Z. Wang, Z. Zhu, M. Fang, Z. Li, J. Xu, Y. He, N. Zhang, Bioact. Mater. 37 (2024) 1.
[101] J.C. Park, S. Park, S. Bang, H. Kim, Y. Lee, M.G. Park, S.G. Yoon, Y. Jeong, H. Kim, S.H. Kang, K.H. Lee, Chem. Eng. J. 506 (2025) 159806.
[102] S. Cai, T. Pataillot-Meakin, A. Shibakawa, R. Ren, C.L. Bevan, S. Ladame, A. P. Ivanov, J.B. Edel, Nat. Commun. 12 (2021) 3515.
[103] C. Koch, B. Reilly-O'Donnell, R. Gutierrez, C. Lucarelli, F.S. Ng, J. Gorelik, A. P. Ivanov, J.B. Edel, Nat. Nanotechnol. 18 (2023) 1483.
[104] S. Kocabey, G. Chiarelli, G.P. Acuna, C. Ruegg, Biosens. Bioelectron. 224 (2023) 115053.
[105] W. Li, W. Wang, S. Luo, S. Chen, T. Ji, N. Li, W. Pan, X. Zhang, X. Wang, K. Li, Y. Zhang, X. Yan, J. Nanobiotechnol. 21 (2023) 328.
[106] J. Ma, Q. Yao, S. Lv, J. Yi, D. Zhu, C. Zhu, L. Wang, S. Su, J. Nanobiotechnol. 22 (2024) 596.
[107] G. Kaur, M. Tintelott, M. Suranglikar, A. Masurier, X.-T. Vu, G. Gines, Y. Rondelez, S. Ingebrandt, Y. Coffinier, V. Pachauri, A. Vlandas, Biosens. Bioelectron. 257 (2024) 116311.
[108] M. Deng, Z. Ren, H. Zhang, Z. Li, C. Xue, J. Wang, D. Zhang, H. Yang, X. Wang, J. Li, Adv. Sci. 10 (2023) 2205886.
[109] R.G. Mahmudunnabi, M. Umer, K.-D. Seo, D.-S. Park, J.H. Chung, M.J. A. Shiddiky, Y.-B. Shim, Biosens. Bioelectron. 207 (2022) 114149.
[110] J. Guo, Y. Zhu, P. Miao, Nano Lett. 23 (2023) 11099.
[111] X. Liu, R. Singh, G. Li, C. Marques, B. Zhang, S. Kumar, J. Lightwave Technol. 41 (2023) 7432.
[112] X. Li, R. Singh, B. Zhang, S. Kumar, G. Li, Photonics Res. 13 (2025) 698.
[113] S. Zhao, Y. Jia, A. Wang, J. Yang, L. Yang, Biosens. Bioelectron. 239 (2023) 115613.
[114] B. Tao, B. Gao, F. Miao, Y. Chen, L. Liu, IEEE Sens. J. 24 (2024) 25627.
[115] X. Hui, C. Yang, D. Li, X. He, H. Huang, H. Zhou, M. Chen, C. Lee, X. Mu, Adv. Sci. 8 (2021) 2100583.
[116] T. Špringer, Z. Krejčík, J. Homola, Biosens. Bioelectron. 194 (2021) 113613.
[117] K. Wang, H. Yin, S. Li, Y. Wan, M. Xiao, X. Yuan, Z. Huang, Y. Gao, J. Zhou, K. Guo, J. Wang, Biosens. Bioelectron. 267 (2025) 116825.
[118] C. Wang, W. Ma, T. Jia, X. Zhang, X. Fan, Sens. Actuators B: Chem. 422 (2025) 136452.
[119] J. Xu, Y. Liu, K.-J. Huang, R. Wang, J. Li, Chem. Eng. J. 466 (2023) 143230.
[120] K.P. Ameya, D. Sekar, Biotechnol. Sustain. Mater. 2 (2025) 6.
[121] N.B. Nafari, M. Zamani, B. Mosayyebi, Clin. Chim. Acta 567 (2025) 120096.
[122] H. Su, X. Liu, Y. Zhu, T. Luowu, H. Sun, T. Zhang, Q. Shi, S. Lu, B. Zhang, M. Yang, J. Guo, B. Shi, Z. Guo, X. Meng, J. Chen, Q. Zhang, Chem. Eng. J. 524 (2025) 169354.
[123] H. Li, H. Xu, Y. Li, X. Li, TrAC Trends Anal. Chem. 174 (2024) 117700.
[124] J. Zhang, M. Lang, Y. Zhou, Y. Zhang, Trends Genet. 40 (2024) 94.
[125] G.A.D. Metcalf, Oncogene 43 (2024) 2135.
[126] Q. Jiang, Q. Mo, C. Ge, W. Li, J. Mai, Y. Chen, Y. Liu, X. Deng, Z. Yang, D. Wang, S. De Matteis, Med. 3 (2025) e20240135.
[127] W. Wang, Y. Xing, L. Liu, M. Wu, P. Huang, B. Li, Z. Wu, ACS Sens. 10 (2025) 310.
[128] X. Ma, L. Chen, Y. Yang, W. Zhang, P. Wang, K. Zhang, B. Zheng, L. Zhu, Z. Sun, S. Zhang, Y. Guo, M. Liang, H. Wang, J. Tian, Front. Bioeng. Biotechnol. 7 (2019), 2019.
[129] N. Khandan-Nasab, S. Askarian, A. Mohammadinejad, S.H. Aghaee-Bakhtiari, T. Mohajeri, R. Kazemi Oskuee, Anal. Biochem. 633 (2021) 114406.
[130] W. Wang, L. Liu, J. Zhu, Y. Xing, S. Jiao, Z. Wu, ACS Nano 18 (2024) 6266.
[131] X. Zhan, Y. Jiang, Z. Li, X. Hu, F. Lan, B. Ying, Y. Wu, ACS Nano 19 (2025) 22849.
[132] A. Zabelina, A. Trelin, A. Skvortsova, D. Zabelin, V. Burtsev, E. Miliutina, V. Svorcik, O. Lyutakov, Anal. Chim. Acta 1278 (2023) 341708.
[133] J. Xu, X. Luo, H. Chen, B. Guo, Z. Wang, F. Wang, ACS Nano 19 (2025) 8812.
[134] Q. Huang, K. Wang, Y. Wang, Talanta 273 (2024) 125928.
[135] M. Yu, Y. Wang, J. Shang, Q. Zhang, Y. Jiang, X. Liu, F. Wang, Nano Today 61 (2025) 102563.
[136] S. Yu, S. Zhao, Y. Liu, T. Gu, S.-H. Wen, J. Ma, Y. Dang, J.-J. Zhu, Y. Zhou, Biosens. Bioelectron. 279 (2025) 117422.
[137] Y. Liang, D. Chen, H. Wang, H. Pian, W. Liu, F. Wang, H. Wang, Z. Li, Biosens. Bioelectron. 238 (2023) 115578.
[138] D. Mao, M. Zheng, W. Li, Y. Xu, C. Wang, Q. Qian, S. Li, G. Chen, X. Zhu, X. Mi, Biosens. Bioelectron. 204 (2022) 114077.
[139] Y. Feng, Q. Liu, X. Zhao, M. Chen, X. Sun, H. Li, X. Chen, Anal. Chem. 94 (2022) 2934.
[140] D. Wu, L. Kang, J. Tian, Y. Wu, J. Liu, Z. Li, X. Wu, Y. Huang, B. Gao, H. Wang, Z. Wu, G. Qiu, Int. J. Nanomed. 15 (2020) 7979.
[141] Y. Sun, P. Miao, J. Wang, Y. Sun, Y. Lv, J. Zhang, M. Yan, Sens. Actuators B: Chem. 422 (2025) 136607.
[142] T.W. Nam, Y. Park, Y.S. Jung, H.G. Park, ACS Nano 16 (2022) 11115.
[143] C.S.M. Martins, A.P. LaGrow, J.A.V. Prior, ACS Sens. 7 (2022) 1269.
[144] F. Lou, B. Guo, J. Dai, J. Wang, F. Yi, S. Shen, C. Cong, G. Hu, J. Jiang, R. Zhang, Y. Lu, ACS Nano 19 (2025) 20108.
[145] A. Khodadoust, N. Nasirizadeh, S.M. Seyfati, R.A. Taheri, M. Ghanei, H. Bagheri, Talanta 252 (2023) 123863.
[146] H. Li, Y. Zhang, G. Jie, Sens. Actuators B: Chem. 339 (2021) 129847.
[147] Y. Wang, H. Feng, K. Huang, J. Quan, F. Yu, X. Liu, H. Jiang, X. Wang, Biosens. Bioelectron. 215 (2022) 114572.
[148] S. Xu, Y. Chang, Z. Wu, Y. Li, R. Yuan, Y. Chai, Biosens. Bioelectron. 149 (2020) 111848.
[149] Y. Gao, S. Xu, T. He, J. Li, L. Liu, Y. Zhang, S. Ge, M. Yan, H. Liu, J. Yu, Sens. Actuators B: Chem. 324 (2020) 128693.
[150] A. Roychoudhury, J.W. Dear, T.T. Bachmann, Biosens. Bioelectron. 212 (2022) 114404.
[151] Adrian M. Molina Vargas, S. Sinha, R. Osborn, Pablo R. Arantes, A. Patel, S. Dewhurst, Dwight J. Hardy, A. Cameron, G. Palermo, Mitchell R. O'Connell, Nucleic Acids Res. 52 (2023) 921.
[152] M.-L. Lu, W. Huang, S. Gao, J.-L. Zhang, W.-B. Liang, Y. Li, R. Yuan, D.-R. Xiao, Anal. Chem. 94 (2022) 15832.
[153] M. Hu, L. Zhu, Z. Li, C. Guo, M. Wang, C. Wang, M. Du, Appl. Surf. Sci. 542 (2021) 148586.
[154] X. Li, Y. Lu, Y. Chen, Z. Pan, N. Lin, Z. Lin, H. Chen, Sens. Actuators B: Chem. 377 (2023) 133035.
[155] T. Qi, C. Song, J. He, W. Shen, D. Kong, H. Shi, L. Tan, R. Pan, S. Tang, H.K. Lee, Anal. Chem. 92 (2020) 5033.

Update

Trends in Analytical Chemistry
Volume 196, Issue , March 2026, Page

DOI: https://doi.org/10.1016/j.trac.2026.118658

Trends in Analytical Chemistry 196 (2026) 118658

Contents lists available at ScienceDirect

Trends in Analytical Chemistry

journal homepage: www.elsevier.com/locate/trac

Corrigendum

Corrigendum to towards clinical application: Emerging strategies for ultrasensitive and selective miRNA detection [TrAC Trends Anal. Chem. 195, (2026) 118593]

Yuhan Wang [a], Zijian Liu [a], Hen-Wei Huang [b], Jung Seung Lee [c], Kexin Liu [a], Mengru Yu [a], Xiaoyue Qi [a,*]

[a] School of Medical Technology, Beijing Institute of Technology, Beijing, 100081, China
[b] School of Electrical & Electronic Engineering, Nanyang Technological University, Singapore, 639798, Singapore
[c] Department of MetaBioHealth, Sungkyunkwan University, Suwon, 16419, Republic of Korea

The authors regret an error occurred in the funding details. The number for the Beijing Natural Science Foundation was stated incorrectly and should be revised. We confirm that the correct grant number is 7244520.

The authors would like to apologise for any inconvenience caused.

DOI of original article: https://doi.org/10.1016/j.trac.2025.118593.
* Corresponding author.
E-mail address: qixiaoyue@bit.edu.cn (X. Qi).

https://doi.org/10.1016/j.trac.2026.118658

Available online 22 January 2026